

The Elements of Temporal Sentence Grounding in Videos: A Survey and Future Directions

Hao Zhang, Aixin Sun, Wei Jing, and Joey Tianyi Zhou

Abstract—Temporal sentence grounding in videos (TSGV), *a.k.a.*, natural language video localization (NLVL) or video moment retrieval (VMR), aims to retrieve a temporal moment that semantically corresponds to a language query from an untrimmed video. Connecting computer vision and natural language, TSGV has drawn significant attention from researchers in both communities. This survey attempts to provide a summary of fundamental concepts in TSGV and current research status, as well as future research directions. As the background, we present a common structure of functional components in TSGV, in a tutorial style: from feature extraction from raw video and language query, to answer prediction of the target moment. Then we review the techniques for multimodal understanding and interaction, which is the key focus of TSGV for effective alignment between the two modalities. We construct a taxonomy of TSGV techniques and elaborate methods in different categories with their strengths and weaknesses. Lastly, we discuss issues with the current TSGV research and share our insights about promising research directions.

Index Terms—Temporal Sentence Grounding in Video, Natural Language Video Localization, Video Moment Retrieval, Temporal Video Grounding, Multimodal Retrieval, Cross-modal Video Retrieval, Multimodal Learning, Video Understanding, Vision and Language.

1 INTRODUCTION

VIDEO has gradually become a major type of information transmission media, thanks to the fast development and innovation in communication and media creation technologies. A video is formed from a sequence of continuous image frames possibly accompanied by audio and subtitle. Compared to image and text, video conveys richer semantic knowledge, as well as more diverse and complex activities. Despite strengths of video, searching for contents from video is challenging. Thus, there is a high demand of techniques that could quickly retrieve video segments of user interest, specified in natural language.

1.1 Definition and History

Given an untrimmed video, temporal sentence grounding in videos (TSGV) is to retrieve a video segment, also known as a temporal moment, that semantically corresponds to a query in natural language *i.e.*, sentence. Illustrated in Fig. 1, for query “A person is putting clothes in the washing machine.”, TSGV needs to return the start and end timestamps (*i.e.*, 9.6s and 24.5s) of a video moment from the input video as answer. The answer moment should contain the actions or events described by the query.

As a fundamental vision-language problem, TSGV also serves as an intermediate step for various downstream vision-language tasks, such as video question answering and video grounded dialogue. These tasks require to localize relevant moments about questions, then discover or generate answer to input question by analyzing the retrieved moments. Naturally, TSGV connects

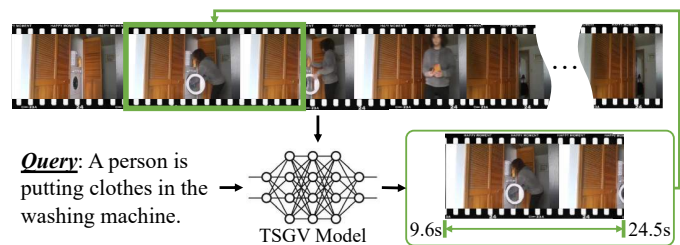


Fig. 1. An illustration of temporal sentence grounding in videos (TSGV).

computer vision (CV) and natural language processing (NLP) communities, and benefits from advancements made in both areas.

TSGV also shares similarities with some classic tasks in both CV and NLP. For instance, video action recognition (VAR) [1]–[4] in CV is to detect video segments, which perform specific actions, from video. Although VAR localizes temporal segments with activity information, it is constrained by the predefined action categories. TSGV is more flexible, and aims to retrieve complicated and diverse activities from video via arbitrary language queries. In this sense, TSGV needs semantic understanding of both video and language, and the multimodal interaction between them. TSGV is similar to reading comprehension (RC) task in NLP [5]–[8], which is to retrieve a span of words from text to answer a question. The core of RC is the interaction between text passage and query. TSGV models the interaction between two different modalities, making it more arduous and challenging.

TSGV was proposed in 2017 [9], [10]; the task immediately drew significant attentions from researchers. Early solutions mainly adopt an ineffective two-stage approach, first to sample moments as candidate answers, then to score these candidates [9]–[13]. Subsequent solutions focus more on effective and efficient multimodal interactions between video and query. A lot of methods are developed, including proposal-based [14]–[18], proposal-free [19]–[23], reinforcement learning-based [24]–[26],

- H. Zhang is with Centre for Frontier AI Research (CFAR), A*STAR, Singapore, 138632, and School of Computer Science and Engineering, Nanyang Technological University, Singapore, 639798.
- A. Sun is with S-Lab, Nanyang Technological University, Singapore, 639798.
- W. Jing is with Alibaba Group, China, 311121.
- J.T. Zhou is with Centre for Frontier AI Research (CFAR), A*STAR, Singapore, 138632.
- Corresponding author: A. Sun (Email: axsun@ntu.edu.sg).

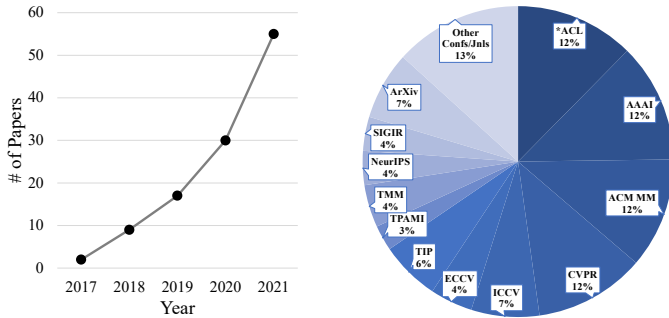


Fig. 2. Statistics of the collected papers in this survey. Left: number of papers published in each year. Right: distribution of papers by venue, where *ACL denotes the series of conferences hosted by the Association for Computational Linguistics.

and weakly-supervised [27]–[31] methods, etc.

In this survey, we aim to provide a comprehensive and systematic review of TSGV research. We collect papers from reputable conferences and journals in CV, NLP, MM, IR, and machine learning areas, *e.g.*, CVPR, ECCV, ICCV, WACV, BMVC, ACL, EMNLP, NAACL, SIGIR, ACM MM, NeurIPS, AACL, IJCAI, and TPAMI, TMM, TIP, etc. The papers were mainly published from 2017 to 2021. For paper collection, we primarily rely on academic search engines and digital libraries, such as IEEE Xplore, ACM Digital Library, ScienceDirect, Springer, ACL Anthology, CVF Open Access, etc. We also adopt Google Scholar to collect papers in other conferences/journals, and open-sourced articles.¹ Fig. 2 summarizes the statistics of the collected papers.

1.2 The User’s Dilemma and the Role of Expertise

The availability of a vast collection of TSGV methods easily confounds a researcher or practitioner attempting to select or design an algorithm suitable for a specific problem at hand. Existing surveys [32]–[34] summarize progress of TSGV research, and establish taxonomies of methods based on their task formulations and architectures. Being the first survey, the taxonomy presented in Yang *et al.* [32] is relatively incomplete and coarse. Liu *et al.* [33] propose a pipeline of TSGV model by partitioning it into three components, and categorize existing solutions into supervised and weakly-supervised groups. However, their taxonomy is also unable to well cover various TSGV approaches. Lan *et al.* [34] present a more complete taxonomy, with detailed illustration and comparison between different categories of methods. Benchmark datasets and evaluation metrics are also covered.

Our survey covers more recent development in TSGV research. By abstracting to common generalities in all methods, we summarize the different types of TSGV methodologies and reveal a common pipeline of TSGV model. We also establish a more comprehensive taxonomy, and conclude more concrete and promising future research directions. All existing surveys focus on summarizing existing TSGV methods and stating future research directions. However, they do not provide critical analysis of existing TSGV methods. More importantly, common questions from researchers/practitioners are not well addressed in existing

1. A number of keywords and their combinations are utilized for paper searching, including moment, grounding, localization, language query, video retrieval, moment retrieval, video grounding, temporal grounding, moment localization, video localization, temporal localization, temporal language grounding, temporal sentence grounding, etc.

surveys: (i) How should TSGV data be processed? (ii) How should data be used in a particular TSGV method? (iii) What does a TSGV method generally look like and how it works? and (iv) Which model assessment is appropriate to use for a particular TSGV method? Our aim is to provide these perspectives on the composition of TSGV methods and the state of the art in TSGV research. With such perspectives, an informed practitioner is able to confidently assess the trade-offs of various TSGV methods and make a competent decision on designing a TSGV solution with a suite of techniques.

This survey is organized as follows. In Section 2, we present a general pipeline of TSGV methods and interpret technical details in a tutorial style. It provides readers background on what a TSGV model looks like generally, its I/O and functional components. Section 3 summarizes major benchmark datasets and evaluation metrics. Section 4 classifies TSGV solutions into categories, elaborates methods in each category, and discusses their pros and cons. Section 5 summarizes current research progress via performance comparisons. Section 6 discusses open issues and further research directions. Section 7 concludes this paper.

2 BACKGROUND

There are no theoretical guidelines that reveal a common structure or pipeline of a TSGV method. Despite various sophisticated architectures in different methods, conceptually, a TSGV method generally contains six components shown in Fig. 3. The dotted line in the figure indicates that proposal generator is an optional component, and it may be placed at different stages. We brief these main components to provide necessary background to readers, before we zoom into the technical details in Section 4.

A TSGV method takes a video-query pair as input, where the video is a collection of consecutive image frames, and the query is a sequence of words. The preprocessor prepares inputs for feature extraction, *e.g.*, downsampling and resizing image frames in video, and tokenizing words in query sentence. Feature extractor converts the video frames and query words into their corresponding vector feature representations. Then the encoder module maps video and query features to same dimension, and aggregates contextual information to enhance the feature representations. The interactor module, an essential component in TSGV, learns the multimodal representations by modeling the cross-modal interaction between video and query. Finally, answer predictor generates moment predictions based on the learned multimodal representations. For proposal-based methods, answer predictor makes predictions based on the proposals generated by proposal generator. A proposal can be considered as a candidate answer moment, which can be generated at different stages. An example proposal is a video segment sampled from the input video. Proposal-free methods predict answers directly without the need of generating candidate answers.

Before we elaborate details of each component, we define the following notations. Given a TSGV dataset, we denote its video corpus as $\mathcal{V} = \{V^1, V^2, \dots, V^N\}$ and its query set as $\mathcal{Q} = \{Q^1, Q^2, \dots, Q^M\}$, where N and M are the number of videos and queries, respectively. Note that, multiple queries can be posed to the same video with its different moments as answers; typically $M \geq N$ in TSGV datasets. Given a video-query pair, a video V contains T frames $V = [f_1, f_2, \dots, f_T]$ and a query Q has m words $Q = [q_1, q_2, \dots, q_m]$, the start and end time of the ground-truth moment are denoted by τ_s and τ_e , $1 \leq \tau_s < \tau_e \leq T$. Here,

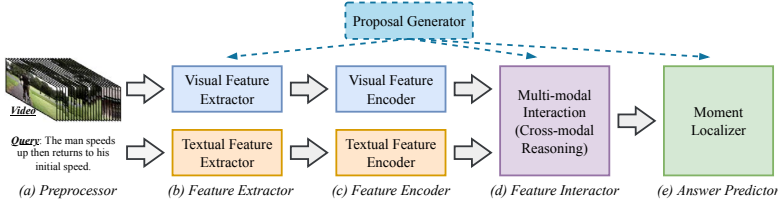


Fig. 3. A general pipeline for temporal sentence grounding in videos.

we use frame index to represent time points, based on a fixed frame rate or fps. Mathematically, TSGV is to retrieve the target moment starting from τ_s and ending at τ_e by giving a video V and query Q , *i.e.*, $\mathcal{F}_{TSGV} : (V, Q) \mapsto (\tau_s, \tau_e)$.

2.1 Preprocessor

Video is a series of still images and the number of frames can be very large. For instance, a 2-minute video with 20 fps has 2,400 frames in total. Thus, it is infeasible (and often unnecessary) to process every frame in a video due to computational cost. On the other hand, video is continuous, *i.e.*, changes between consecutive frames are usually small and smooth. Hence it is reasonable to downsample video for efficient computation. As illustrated in Fig. 4, if we sample 1 frame from every 20 consecutive frames, we only need to process 120 frames instead of 2400 frames for this 2-minute video. With a downsample rate r_{ds} , the number of video frames becomes $T' = T/r_{ds}$. Downsample rate has a direct impact on video quality, and should be carefully selected depending on the dataset.

Language query is discrete and words in a sentence demonstrate syntactic structure. Different word combinations lead to very different semantic meanings. For instance, given a query sentence “The man speeds up then returns to his initial speed.”, the words “initial” and “speed” carry different meanings, and their combination describes a specific scene. For preprocessing, query is typically tokenized into word tokens. If a query contains too many words, a common strategy is truncation, *i.e.*, taking a fixed number of words from beginning and discarding the rest.

2.2 Feature Extractor

The feature extractor bridges the raw inputs and the model by converting inputs into feature representations.

Textual Feature Extractor maps a query sentence to an embedding space, which can be categorized into token-level and sentence-level extractors. Token-level extractor converts each word into its corresponding word embedding by using pre-trained word embeddings (PWE), *e.g.*, Word2Vec [35] and GloVe [36], or pre-trained language models (PLM), *e.g.*, BERT [37] and RoBERTa [38]. We represent token-level extraction as:

$$Q = [q_1, \dots, q_m] \xrightarrow{\text{PWE/PLM}} \mathbf{Q} = [\mathbf{q}_1, \dots, \mathbf{q}_m] \in \mathbb{R}^{m \times d_q}, \quad (1)$$

where d_q denotes word embedding dimension.

Sentence-level extractor encodes the entire query into a sentence feature in d_s dimension, by using pre-trained sentence encoder (PSE), *e.g.*, Skip-Thought [39], InferSent [40], SentenceBERT [41], or PWE/PLM with a trainable sentence encoder (TSE). We represent the process as:

$$Q = [q_1, \dots, q_m] \xrightarrow{\text{PSE}} \mathbf{q}_s \in \mathbb{R}^{d_s}, \text{ or} \quad (2)$$

$$Q = [q_1, \dots, q_m] \xrightarrow{\text{PWE/PLM}} \mathbf{Q} \in \mathbb{R}^{m \times d_q} \xrightarrow{\text{TSE}} \mathbf{q}_s \in \mathbb{R}^{d_s}$$

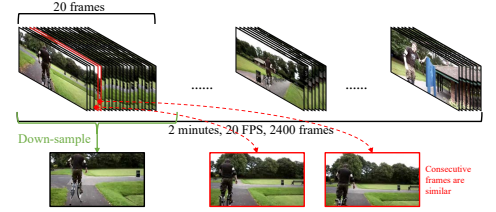


Fig. 4. An example of video frames down-sampling.

Visual Feature Extractor converts video frames into a sequence of visual features. Depending on whether proposals are generated directly on input video, there are two types of feature extraction.

Recall that a proposal is a candidate answer. A straightforward approach is to sample video segments from input video as proposals. Proposals may contain different number of frames. Suppose there are n_{seg} video segments as proposals, the feature extraction process is described as:

$$V \in \mathbb{R}^{T' \times \text{frame}} \xrightarrow{\text{proposals}} \{\text{segment}_i \in \mathbb{R}^{\chi \times \text{frame}}\}_{i=1}^{n_{\text{seg}}} \quad (3)$$

$$\xrightarrow{\text{visual feature extractor}} \mathbf{V} = \{\mathbf{v}_{p,i} \in \mathbb{R}^{d_v}\}_{i=1}^{n_{\text{seg}}},$$

where χ is the number frames in a proposal, and d_v denotes the dimension of extracted features. The task becomes to determine whether a proposal represented by $\mathbf{v}_{p,i}$ is the correct answer.

If proposals are not generated directly from input video, then the video is uniformly decomposed into a sequence of non-overlapping snippets. Suppose there are n_{snp} video snippets and each snippet contains ξ frames, the extraction process is:

$$V \in \mathbb{R}^{T' \times \text{frame}} \xrightarrow{\text{decompose}} [\text{snippet}_i]_{i=1}^{n_{\text{snp}}} \in \mathbb{R}^{n_{\text{snp}} \times \xi \times \text{frame}} \quad (4)$$

$$\xrightarrow{\text{visual feature extractor}} \mathbf{V} = [\mathbf{v}_i]_{i=1}^{n_{\text{snp}}} \in \mathbb{R}^{n_{\text{snp}} \times d_v}.$$

Here we distinguish “video snippet” from “video segment”. Video segment is sampled as a proposal to match the target moment, and video snippet is a very short clip which only contains a few frames, *i.e.*, $\xi \ll \chi$ in general. Further, as each video segment is one candidate answer, video segments are irrelevant to each other and they are further processed separately in TSGV. As very short clips, video snippets are maintained in a sequence, and are jointly processed in later stages.

Each frame is a still image. From video frames to features, the commonly used visual feature extractor are (i) 3D-based ConvNet pre-trained for action recognition, *e.g.*, C3D [1] or I3D [3], and (ii) 2D-based ConvNet pre-trained for object detection, *e.g.*, VGG [42] or ResNet [43].

2.3 Feature Encoder and Feature Interactor

Feature encoder maps visual and textual features to the same dimension, and refines their feature representations by encoding their corresponding contextual information. Existing TSGV methods use various feature encoders, from simple multi-layer perceptrons to complex transformers and graph neural networks. The design of feature encoder highly depends on model architecture.

Briefed in Section 2.1, there are token-level and sentence-level query features. There are also two types of visual features, depending on whether proposal generator is applied on input video, *i.e.*, proposal feature and video snippet feature sequence. Let d be the

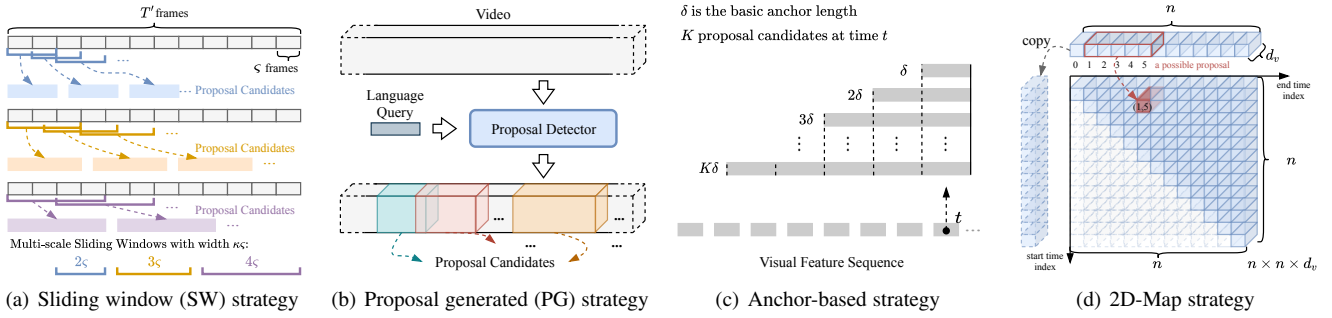


Fig. 5. Illustration of sliding window, proposal generated, anchor-based, and 2D-Map strategies.

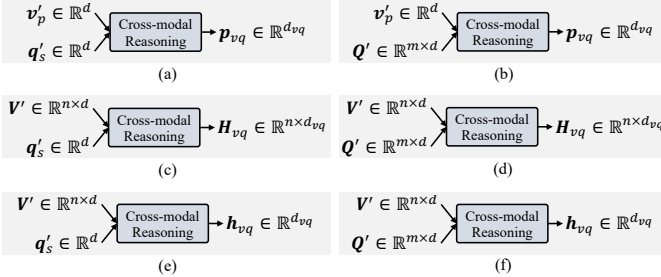


Fig. 6. The common input/output feature formats of feature interactor in TSGV. $\mathbf{p}_{vq} \in \mathbb{R}^{d_{vq}}$ denotes the learned multimodal proposal feature; $\mathbf{H}_{vq} = [\mathbf{h}_{vq}^1, \dots, \mathbf{h}_{vq}^n] \in \mathbb{R}^{n \times d_{vq}}$ is the multimodal snippet feature sequence; $\mathbf{h}_{vq} \in \mathbb{R}^{d_{vq}}$ is the pooled multimodal snippet feature. d_{vq} denotes the dimension of output multimodal feature.

target dimension for both visual and textual features. Mapping of sentence-level and token-level query features is defined as:

$$\begin{aligned} \mathbf{q}_s \in \mathbb{R}^{d_s} &\xrightarrow[\text{encoder}]{\text{textual feature}} \mathbf{q}'_s \in \mathbb{R}^d, \text{ and} \\ \mathbf{Q} \in \mathbb{R}^{m \times d_q} &\xrightarrow[\text{encoder}]{\text{textual feature}} \mathbf{Q}' \in \mathbb{R}^{m \times d}. \end{aligned} \quad (5)$$

For proposal feature and video snippet feature sequence, the mapping is written as:

$$\begin{aligned} \mathbf{v}_p \in \mathbb{R}^{d_v} &\xrightarrow[\text{encoder}]{\text{visual feature}} \mathbf{v}'_p \in \mathbb{R}^d, \text{ and} \\ \mathbf{V} \in \mathbb{R}^{n \times d_v} &\xrightarrow[\text{encoder}]{\text{visual feature}} \mathbf{V}' \in \mathbb{R}^{n \times d}, \end{aligned} \quad (6)$$

where we simply use $\mathbf{v}_p \in \mathbb{R}^{d_v}$ to represent the visual feature of a proposal, and n to replace n_{snp} .

Feature interactor, an essential component in any TSGV method, aims to learn cross-interaction between video and query. Recall the goal of TSGV is to retrieve a target moment from video that *semantically corresponds* to the query. Thus, feature interactor requires to understand the semantic meaning of query, and to recognize various activities in the video simultaneously. It then performs to fuse query and video representations by emphasizing the portion of video content that is most relevant to the query semantics. In general, quality of feature interactor determines the performance of a TSGV method to a large extent.

Fig. 6 summarizes the various input and output formats of different feature interactors among existing TSGV methods. The input is determined by the types of query features (token-level or sentence-level), and the types of visual features (proposal or snippet sequence). The common output feature formats include (i) the learned multimodal proposal feature $\mathbf{p}_{vq} \in \mathbb{R}^{d_{vq}}$, (ii) the

multimodal snippet feature sequence $\mathbf{H}_{vq} = [\mathbf{h}_{vq}^1, \dots, \mathbf{h}_{vq}^n] \in \mathbb{R}^{n \times d_{vq}}$, and (iii) the pooled multimodal snippet feature $\mathbf{h}_{vq} \in \mathbb{R}^{d_{vq}}$. Here, d_{vq} is the dimension of the multimodal feature.

Output format of feature interactor is highly correlated to the answer predictor in a TSGV method. Answer predictor may depend on proposals that can be generated at different stages. We next brief proposal generation, before answer predictor.

2.4 Proposal Generation

Depending on whether a proposal generation module is used, existing TSGV methods can be roughly categorized into *proposal-based* and *proposal-free* methods. As shown in Fig. 3, proposal generator can be integrated into the model at various positions. For instance, proposals can be directly sampled from the input video. Proposals can also be generated before or after feature interactor based on the visual features. Anchor-based methods generate proposals during answer prediction. A method may also engage multiple proposal generation strategies.

Sliding window-based (SW) strategy [9]–[11], [13], [44] generates proposal candidates by densely sampling fixed-length video segments on input video, using pre-defined multi-scale sliding windows. SW strategy is usually performed directly on video frames. Illustrated in Fig. 5(a), given a downsampled video with T' frames and a set of sliding windows, each sliding window samples video segments sequentially, with a preset overlap ratio. In our illustration, we use three different sliding windows $sw \in \{\kappa\varsigma\}_{\kappa=2,3,4}$ (ς denotes a basic window size) and set the overlap ratio as 0.5. Overlap ratio is necessary to increase the chance of covering target moment. Then we have a set of video segments as proposals.

Proposal-generated (PG) strategy [14], [45]–[48] produces proposals by utilizing auxiliary modules, *e.g.*, a pre-trained segment proposal network (SPN) [49] or a carefully designed proposal detector. The PG strategy is usually performed on visual features, but it involves the query as input to guide its proposal generation process, illustrated in Fig. 5(b). Hence, the proposal generated are related to the query. Depending on the position of proposal detector, PG strategy may also involve feature encoder and interactor.

Anchor-based strategy [15]–[17], [50], [51] generates proposals with pre-set multi-scale anchors. Different from SW strategy, it is performed on the encoded visual features and is integrated in answer predictor. Suppose we have K different scale anchors, and the length of a basic anchor is δ . Fig. 5(c) plots a commonly used anchor-based strategy. This strategy applies K preset anchors to

generate proposals, ended at a time step t , where t is the index of multimodal visual feature in the feature sequence.

Another version of anchor-based strategy is 2D-Map strategy [18], [52]–[55]. Different from the standard anchor-based strategy above, 2D-Map strategy is usually applied after feature extractor, *i.e.*, before answer predictor. It generates proposals by modeling the temporal relations between video moments through a two-dimensional map. One dimension indicates the starting time of a moment; the other indicates the end time. Given a visual feature sequence with $n \times d_v$, all possible proposal candidates are computed based on a 2D temporal feature map. Shown in Fig. 5(d), a candidate proposal representation can be computed by max-pooling the corresponding visual features across the specific time span, resulting in the 2D feature map with $n \times n \times d_v$. Note the start (a) and end (b) timestamps of a proposal candidate should satisfy $a \leq b$. Therefore, only proposal candidates that locate in the upper triangular part of the 2D map are valid.

2.5 Answer Predictor and Objective

Answer predictor is responsible for predicting the position of a target moment based on the learned multimodal features. Next, we brief the commonly used answer predictors and their corresponding objectives, for both proposal-based and proposal-free methods. Methods may combine multiple answer predictors or incorporate various auxiliary objectives to boost performance. In this background section, we only focus on the main objectives.

For proposal-based methods, answer predictor computes a score for each proposal. Ideally, a proposal gets a higher score if it is closer to ground-truth moment. Specifically, given a multimodal proposal feature \mathbf{p}_{vq} , its score is computed as $s = \sigma(\mathcal{A}(\mathbf{p}_{vq})) \in \mathbb{R}^1$, where \mathcal{A} denotes the answer predictor and σ is an (optional) activation function. Then, the proposal with highest score is selected as the answer. If the proposals are generated by anchor-based strategy, the score is computed based on the multimodal snippet feature sequence \mathbf{H}_{vq} by applying multi-scale anchors in the answer predictor.

Various learning objectives have been developed for proposal-based methods. The alignment loss is commonly used for SW and PG strategies, defined as:

$$\mathcal{L}_{aln} = \gamma \log(1 + e^{-s_{i,i}}) + \sum_{j=0, j \neq i}^{N_{neg}} \log(1 + e^{s_{i,j}}), \quad (7)$$

where $s_{i,i}$ is the score of aligned (or positive) proposal-query pair, and $s_{i,j}$ is the score of misaligned (or negative) pair; γ is a hyper-parameter to control the weight between positive and negative pairs; N_{neg} represents the number of negative pairs. For a given query, a proposal is considered as positive if it has a good overlap with ground truth moment, measured by IoU (intersection area over union area). Otherwise, the proposal is negative. Nevertheless, a negative pair can also be constructed by replacing a random query or pairing random but unmatched proposals and queries. In general, \mathcal{L}_{aln} encourages aligned proposal-query pairs to have positive scores and misaligned pairs to have negative scores. Besides, triple-based ranking loss has also been used for SW and PG strategies:

$$\mathcal{L}_{triple} = \max(0, \eta + s' - s) \quad (8)$$

where s denotes the score of matched proposal-query pair and s' is the score of mismatch proposal-query pair. Similarly, \mathcal{L}_{triple}

encourages similarities between aligned pairs to be greater than misaligned pairs by some margin $\eta > 0$.

For anchor-based and 2D-Map strategies, binary cross-entropy is usually adopted, defined as:

$$\mathcal{L}_{bce} = \gamma \cdot y \cdot \log s + (1 - y) \cdot \log(1 - s) \quad (9)$$

where γ is an optional balance weight, determined based on the number of positive and negative samples. y is the corresponding anchor label for the proposal; $y = 1$ if the proposal candidate has IoU with ground-truth moment larger than a threshold θ , *i.e.*, positive. Otherwise $y = 0$. y may also be defined as the scaled IoU value between the proposal and ground-truth moment.

Proposal-free methods do not generate proposals. They use a regressor or a span predictor as answer predictor. Specifically, regression-based predictor aims to regress the start and end times of target moment directly. It takes the pooled multimodal snippet feature \mathbf{h}_{vq} as input and predicts the temporal positions (t_s, t_e) . Mathematically, we represent this process as $(t_s, t_e) = \sigma(\mathcal{A}(\mathbf{h}_{vq})) \in \mathbb{R}^2$, where \mathcal{A} denotes the regressor, and σ is (optional) Sigmoid activation to normalize the output to $[0, 1]$. Given a predicted (t_s, t_e) and the normalized ground-truth (τ_s, τ_e) , the smoothed L_1 loss or MSE loss, *i.e.*, $R \in \{\text{smooth}_{L_1}, \text{MSE}\}$, is commonly used as learning objective:

$$\mathcal{L}_{reg} = R(t_s - \tau_s) + R(t_e - \tau_e), \quad (10)$$

Span predictor also predicts the start and end boundaries of target moment directly. Different from regression-based predictor, span predictor computes the probability of each video snippet being the start and end points of target moment. Specifically, it takes the multimodal snippet feature sequence \mathbf{H}_{vq} , and computes the start and end boundary scores as $(\mathbf{S}_s, \mathbf{S}_e) = \mathcal{A}(\mathbf{H}_{vq}) \in \mathbb{R}^{n \times 2}$. Then, the probability distributions of boundaries are computed by $\mathbf{P}_s = \text{softmax}(\mathbf{S}_s) \in \mathbb{R}^n$ and $\mathbf{P}_e = \text{softmax}(\mathbf{S}_e) \in \mathbb{R}^n$, where $\mathbf{P}_{s/e}^t$ denotes the probability of t -th snippet be the start/end boundary. Cross-entropy and Kullback-Leibler (KL) divergence are both commonly used for span prediction. The cross-entropy objective is defined as:

$$\mathcal{L}_{span} = f_{XE}(\mathbf{P}_s, \mathbf{Y}_s) + f_{XE}(\mathbf{P}_e, \mathbf{Y}_e), \quad (11)$$

where f_{XE} is the cross-entropy loss; \mathbf{Y}_s and \mathbf{Y}_e denote the ground-truth labels for start and end boundaries, respectively. $\mathbf{Y}_{s/e}$ is a n -dim one-hot vector, which is generated by setting the index of the snippet contains $\tau_{s/e}$ as 1, and others as 0. Similarly, the KL-divergence objective is defined as:

$$\mathcal{L}_{span} = D_{KL}(\mathbf{P}_s || \hat{\mathbf{Y}}_s) + D_{KL}(\mathbf{P}_e || \hat{\mathbf{Y}}_e), \quad (12)$$

where D_{KL} denotes KL-divergence; $\hat{\mathbf{Y}}_s$ and $\hat{\mathbf{Y}}_e$ are the ground-truth start and end boundary distributions. Not specified in an one-hot $\mathbf{Y}_{s/e}$, the ground-truth boundary distribution is formulated as $\hat{\mathbf{Y}}_{s/e} \sim \mathcal{N}(\tau_{s/e}, \sigma_{std}^2)$, where $\mathcal{N}(\mu, \sigma_{std}^2)$ is the normal distribution with expectation μ and standard deviation σ_{std} .

To summarize, we brief the main components in TSGV methods from input processing to answer prediction. Although existing TSGV methods may contain more sophisticated structures and diverse ancillary modules, their model frameworks generally follow this pipeline. Among the components, the effectiveness of feature interactor highly affects TSGV performance. Proposal generation strategies are highly correlated with the design of answer predictor, and each strategy has its own advantages and drawbacks. Lastly, all methods rely on effective feature extractors, mainly developed in computer vision and natural language processing areas.

TABLE 1
 Statistics of the TSGV benchmark datasets. Different queries may correspond to the same moment.

Dataset	DiDeMo	Charades-STA	ActivityNet Captions	TACoS _{org}	TACoS _{2DTAN}	MAD
Video Source	Flickr	Homes	YouTube	Lab Kitchen		Movie
Domain	Open	Indoor Activity	Open	Cooking		Open
# Videos	10,464	6,672	14,926	127		650
# Moments	26,892	11,767	71,953	3,290	7,069	-
# Queries (or Annotations)	40,543	16,124	71,953	18,818	18,227	384,600
Average # Annotations per Video	3.87	2.42	4.82	148.17	143.52	-
Vocabulary Size	7,785	1,303	15,505	2,344	2,287	61,400
Average Video Length (seconds)	30.00	30.60	117.60	286.59		6,646.20
Min / Max Video Length (seconds)	-	5.50 / 194.33	1.58 / 755.11	48.30 / 1,402.18		-
Average Moment Length (seconds)	-	8.09	37.14	6.10	27.88	4.10
Min / Max Moment Length (seconds)	-	1.68 / 80.80	0.05 / 408.80	0.31 / 166.97	0.48 / 843.20	-
Average Query Length (words)	-	7.22	14.41	10.05	9.42	12.70
Min / Max Query Length (words)	-	3 / 13	4 / 91	2 / 229	2 / 69	-

3 DATASETS AND MEASURES

Datasets are essential resources for building and evaluating TSGV methods. We review benchmark datasets and evaluation metrics.

3.1 Benchmark Datasets

A TSGV dataset typically contains a collection of videos. Each video may come with one or more annotations, *i.e.*, moment-query pairs. Each annotation has a query corresponding to a moment in the video. A few TSGV datasets have been developed, covering various scenarios with distinct characteristics, *e.g.*, different scenes, and activity complexities, summarized in Table 1.²

DiDeMo has its root in YFCC100M [56] dataset, and the latter contains over 100k Flickr videos about various human activities. Hendricks *et al.* [10] randomly select over 14,000 videos, then split and label video segments. Each segment is a five-second video clips, hence the length of ground-truth moment is five seconds. DiDeMo dataset consists of 10,464 videos and 40,543 annotations in total, on average 3.87 annotations per video. Note that, the videos are released in the form of extracted visual features, hence we cannot provide detailed statistics in Table 1. Hendricks *et al.* [57] further collect a TEMPO dataset, which is built on top of DiDeMo, by augmenting more language queries via template model (template language) and human annotators (human language). Compared to DiDeMo, TEMPO contains more complex human-language queries.

Charades-STA is built by Gao *et al.* [9] from the Charades dataset [58]. The Charades dataset contains 9,848 annotated videos about human daily indoor activities for video activity recognition. The original dataset provides 27,847 video-level sentence descriptions, 66,500 temporally localized intervals for 157 action categories, and 41,104 labels for 46 object categories. Based on Charades, Gao *et al.* [9] design a semi-automatic way to construct Charades-STA. They first parse the activity labels from video descriptions using Stanford CoreNLP [59], then match labels with sub-sentences, and finally align sub-sentences with the original label-indicated temporal intervals. In this way, a collection of (sentence query, target moment) pairs are generated as annotations. Because the original descriptions are quite short, Gao *et al.* [9] further combine consecutive descriptions into a

more complex sentence to enhance description complexity for test. Charades-STA contains 6,672 videos and 16,124 annotations. Average video length, moment length, and query length are 30.60 seconds, 8.09 seconds and 7.22 words, respectively.

ActivityNet Captions is developed by Krishna *et al.* [60] for dense video captioning task. However, the sentence-moment pairs in this dataset can naturally be adopted for TSGV task. The videos are taken from ActivityNet [61] dataset, a human activity understanding benchmark. ActivityNet provides samples from 203 activity classes, with an average of 137 untrimmed videos per class and 1.41 activity instances per video [61]. The official test set of ActivityNet Captions is withheld for competition, existing TSGV methods mainly use the official “val1” and/or “val2” development sets as test sets. Thus, statistics of ActivityNet Captions in Table 1 does not consider its official test set. In total, there are 14,926 videos and 71,953 annotations in ActivityNet Captions, where each video contains 4.82 temporally localized sentences on average. Average video and moment lengths are 117.60 and 37.14 seconds, respectively. Average query length is about 14.41 words.

TACoS dataset [62] is selected from the MPII Cooking Composite Activities dataset [63], originally developed for human activity recognition under specific scene, *i.e.*, composite cooking activities in lab kitchen. TACoS contains 127 videos, and each video is associated with two types of annotations: (1) fine-grained activity labels with temporal location, and (2) natural language descriptions with temporal locations. The natural language descriptions are from crowd-sourcing annotators, who describe the video content by sentences [62]. TACoS has 18,818 moment-query pairs. Average video and moment lengths are 286.59 and 6.10 seconds, and average query length is 10.05 words. Each video in TACoS contains 148.17 annotations on average. We name this dataset TACoS_{org} in Table 1. A modified version TACoS_{2DTAN} is made available by Zhang *et al.* [18]. TACoS_{2DTAN} has 18,227 annotations. On average, there are 143.52 annotations per video. The average moment length and query length after modification are 27.88 seconds and 9.42 words, respectively.

MAD [64] is a large-scale dataset containing mainstream movies. Compared to previous datasets, MAD aims to avoid the hidden biases (detailed in Section 6.1) and provide accurate and unbiased annotations for TSGV. Instead of relying on crowd-sourced annotations, Soldan *et al.* [64] adopt a scalable data collection strategy. They transcribe the audio description track of a movie and remove sentences associated with actor’s speech, to obtain highly

2. For DiDeMo and MAD datasets, we directly obtain their statistical results from the original papers. For others, we conduct statistics on raw datasets. We also filter out or modify some invalid annotations in each dataset.

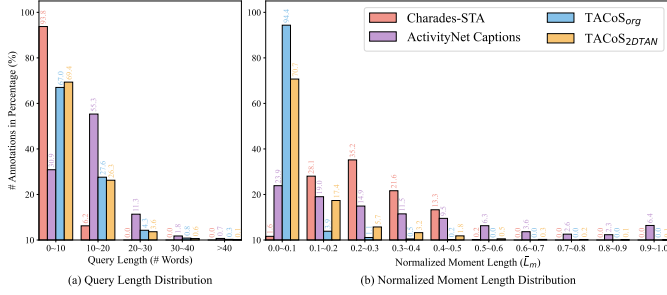


Fig. 7. Statistics of query length and normalized moment length over benchmark datasets.

descriptive sentences that are grounded in long-form videos. MAD contains 650 movies with over 1,200 hours of video length in total. Average video duration is around 110 minutes. Each video in MAD is a full movie without pruning. MAD has 348,600 queries with vocabulary size of 61,400. Average query length is 12.7 words. Average length of temporal moment in MAD is merely 4.1 seconds, making the localization process more challenging.³

Videos in aforementioned datasets may be from open domain or constrained in narrow and specific scenes (see Table 1). Open domain videos contain more diverse and complex activities, making them more challenging, but are closer to real-world scenarios. Although DiDeMo videos are from open domain, answers in this dataset are in fixed-length, *i.e.*, five-second. The fixed-length considerably reduces the complexity of finding answers in DiDeMo.

ActivityNet Captions and DiDeMo have much larger vocabulary size than Charades-STA and TACoS, suggesting that the former two datasets provide rich variations in language queries. From the perspective of query length (see Fig. 7 (a)), a large portion of queries in Charades-STA (93.8%) and TACoS (> 67.0%) has fewer than 10 words. Query length distribution indicates that ActivityNet Captions contain more queries with complicated expressions. Fig. 7 (b) depicts the normalized moment length (\bar{L}_m) distribution, computed against the length of its source video. A small \bar{L}_m means the moment is difficult to retrieve due to moment sparsity [65]. The figure shows more than 70.7% of the moments in TACoS has $\bar{L}_m \leq 0.1$, while 70.1% moments in Charades-STA are in the range of $0.2 < \bar{L}_m \leq 0.5$.

3.2 Evaluation Metrics

TSGV are generally evaluated by comparing predictions with ground-truth annotations. The widely used measures include: mean IoU (mIoU), $\langle R@n, \text{IoU}@m \rangle$, and $\langle dR@n, \text{IoU}@m \rangle$.

Intersection over Union (IoU) is a metric commonly used in object detection [66]–[68] for measuring similarity between two bounding boxes. Hence the standard IoU in object detection is defined on a two-dimensional spatial space. TSGV focuses on temporal dimension only. Thus, temporal IoU is adopted to measure similarity between the ground-truth and predicted moments in TSGV, illustrated in Fig. 8(a). IoU is computed as the ratio of intersection area over union area between two moments, in the range of 0.0 to 1.0. A larger IoU means the two moments match better, and $\text{IoU} = 1.0$ denotes exact match. The mIoU metric

3. At the time of writing, MAD dataset is not publicly available.

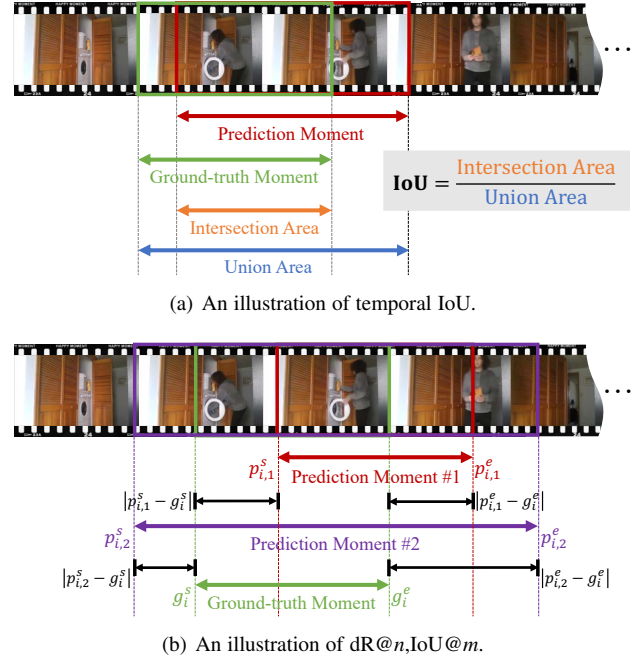


Fig. 8. The temporal intersection over union (IoU), and the discounted- $R@n, \text{IoU}@m$ ($dR@n, \text{IoU}@m$). p_i^s and p_i^e are start and timestamps of predicted moments, g_i^s/e is start/end timestamp of ground-truth moment. $|\cdot|$ denotes absolute operation.

is the average temporal IoUs among all annotations in test set. Mathematically, mIoU is defined as:

$$\text{mIoU} = \frac{1}{N_q} \sum_{i=1}^{N_q} \text{IoU}_i \quad (13)$$

where N_q denotes the total number of annotations or query samples, and IoU_i is the IoU value of i -th sample.

The mIoU is computed based on the single top-ranked prediction for each query. However, given a query, the top-ranked prediction by a TSGV model may not always have the best match with ground-truth. It is reasonable to relax the evaluation by considering top- n retrieved moments for each query. The $\langle R@n, \text{IoU}@m \rangle$ [69] is the percentage of queries, having at least one result whose temporal IoU with ground-truth is larger than m among the top- n retrieved moments. For query q_i , among its top- n retrieved moments, if there exists at least one moment whose IoU with ground-truth is larger than m , then q_i is considered as positive, denoted by $r(n, m, q_i) = 1$. Otherwise, $r(n, m, q_i) = 0$. Thus, $\langle R@n, \text{IoU}@m \rangle$ is calculated as:

$$R@n, \text{IoU}@m = \frac{1}{N_q} \sum_{i=1}^{N_q} r(n, m, q_i) \quad (14)$$

Yuan *et al.* [70] reveal that $\langle R@n, \text{IoU}@m \rangle$ is unreliable on small IoU thresholds. A method tends to generate long predictions if a substantial proportion of ground-truth moments are long in a dataset. In this way, the method increases its chance of correct prediction under small IoU thresholds. Discounted- $R@n, \text{IoU}@m$ ($dR@n, \text{IoU}@m$) is proposed to alleviate this problem [70]. This new measure leverages “temporal distance” between the predicted

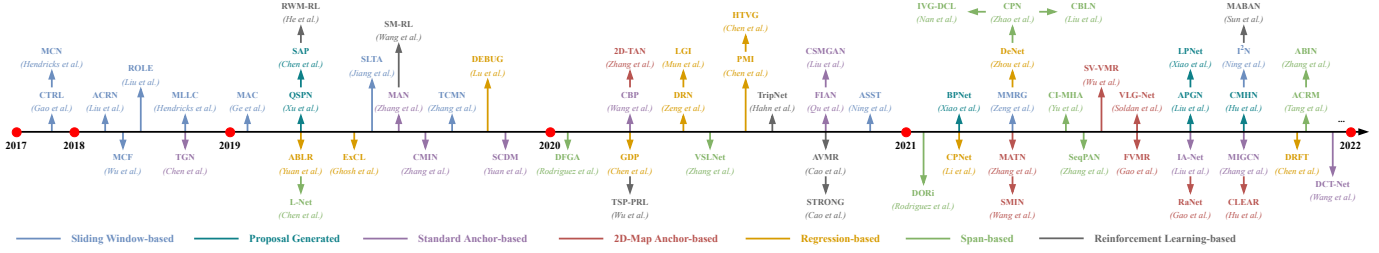


Fig. 9. Chronological overview of selected supervised TSGV methods in different categories. The methods plotted at the same position on the timeline are published in the same venue.

and ground-truth moments to discount $r(n, m, q_i)$ value. $\langle dR@n, IoU@m \rangle$ is calculated as:

$$dR@n, IoU@m = \frac{1}{N_q} \sum_{i=1}^{N_q} r(n, m, q_i) \cdot \alpha_i^s \cdot \alpha_i^e \quad (15)$$

where the discounted ratio $\alpha_i^* = 1 - |p_i^* - g_i^*|$, $*$ $\in \{s, e\}$. $|p_i^* - g_i^*|$ is the absolute distance between the boundaries of predicted and ground-truth moments (see Fig. 8(b)). Note both p_i^* and g_i^* are normalized in 0.0 to 1.0 by dividing the corresponding whole video length. If the predicted moment exactly matches ground-truth, then discounted ratio $\alpha_i^* = 1$, and the metric degrades to $\langle R@n, IoU@m \rangle$. Otherwise, even if IoU threshold is met, $r(n, m, q_i)$ is discounted by α_i^* , which helps to restrain over-long predictions.

In Fig. 8(b), $(p_{i,1}^s, p_{i,1}^e)$ and $(p_{i,2}^s, p_{i,2}^e)$ are two example predicted moments of query q_i , and (g_i^s, g_i^e) is ground-truth moment. Suppose both Predictions 1 and 2 in Fig. 8(b) have the same IoU value which satisfies $IoU \geq m$, ($m \leq 0.5$ here), $\langle dR@n, IoU@m \rangle$ penalizes more on Prediction 2 since its temporal boundaries are farther from ground-truth. With respect to $\langle R@n, IoU@m \rangle$ and $\langle dR@n, IoU@m \rangle$ metrics, community is habituated to set $n \in \{1, 5, 10\}$ and $m \in \{0.3, 0.5, 0.7\}$.

4 TSGV METHODS

Majority solutions proposed for TSGV belong to supervised learning paradigm. Early solutions mainly rely on sliding windows or segment proposal network to pre-sample proposal candidates from input video. Then, the proposals are paired with query to generate best answers through cross-modal matching. However, this two-stage “propose-and-rank” pipeline is inefficient, because densely sampling candidates with overlap is essential to achieve high accuracy, leading to redundant computation and low efficiency. Meanwhile, the pairwise proposal-query matching may also neglect the contextual information. To overcome these drawbacks, alternative solutions like anchor-based and proposal-free methods are developed to address TSGV in an “end-to-end” manner. These methods encode the entire video sequence and all video information are maintained in the model, gradually becoming predominate solutions for TSGV. Fig. 9 depicts a chronological overview of development in supervised learning for TSGV.

Supervised learning requires a large number of annotated samples to train a TSGV method. Considering the difficulty and cost of data annotation, recent studies attempt to solve TSGV with weakly-supervised learning. These methods relieve annotation burden by learning from video-query pairs without the detailed annotation of temporal locations of events in videos.

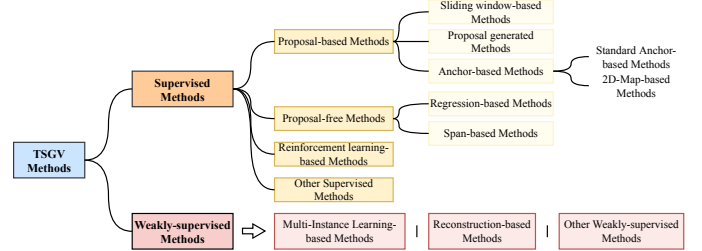


Fig. 10. A taxonomy of methods for TSGV.

Accordingly, the simple classification of proposal-based and proposal-free methods in Section 2 is incapable of well covering all TSGV methods. Based on methods’ architectures and learning algorithms, we propose a new taxonomy in Fig. 10 to categorize TSGV methods. Next, we review solutions to TSGV following this taxonomy and discuss the characteristics for each method category. Because majority are supervised learning solutions, this section is organized mainly based on the categories under supervised learning.

4.1 Proposal-based Method

Depending on the ways to generating proposal candidates, proposal-based methods can be grouped into three categories, *i.e.*, sliding window-based, proposal generated, and anchor-based methods. Sliding window-based and some of proposal generated methods follow a two-stage propose-and-rank pipeline, where the generation of proposal candidates is separated from model computation. Anchor-based methods incorporate proposal generation in model computation to achieve end-to-end learning.

4.1.1 Sliding Window-based Method

Sliding window-based method adopts a multi-scale sliding windows (SW) to generate proposal candidates (ref. Fig. 5(a)). Then multimodal matching module finds the best matching proposal for a query. CTRL [9] and MCN [10] are two canonical SW methods, which are also the pioneering work in TSGV. They define the task and construct corresponding benchmark datasets.

CTRL first produces proposals in various lengths through sliding windows, then encodes these proposals by a visual encoder, shown in Fig. 11. The query is converted to sentence representation via textual encoder. For cross-modal reasoning, it builds a relatively simple multi-modal processing module with three operators, *i.e.*, add, multiply, and fully-connected (FC) layer, to fuse visual and textual features. CTRL designs multi-task objectives by using both alignment predictor and regressor. The

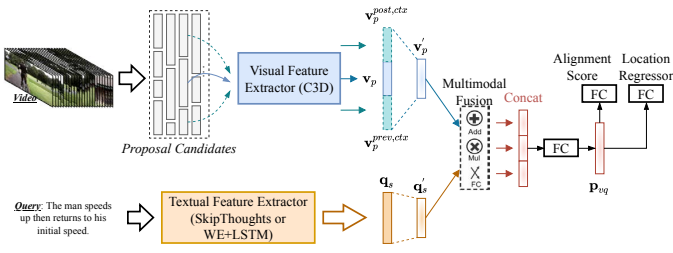


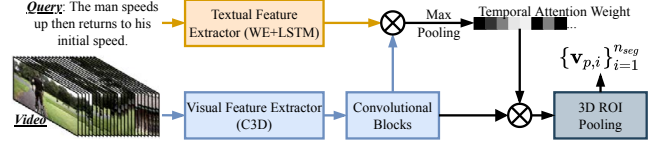
Fig. 11. CTRL architecture, reproduced from Gao *et al.* [9].

alignment predictor computes matching score between proposal and query (ref. Eqn. 7). However, for an aligned proposal-query pair, position of the proposal may not match ground-truth moment exactly. The regressor uses smoothed L_1 loss to compute the corresponding offsets (ref. Eqn. 10) to better align the proposal.

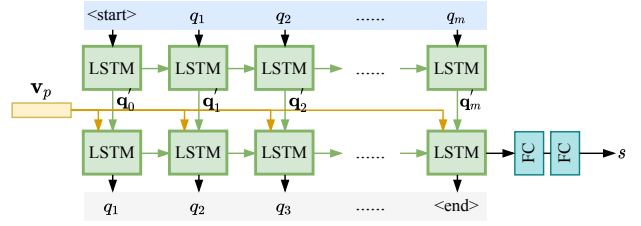
Different from CTRL, MCN aims to project both proposal and query features to a common embedding space. Then, it encourages the distance between query and aligned proposal to be smaller than that of negative proposals, in the shared space. Specifically, MCN minimizes the squared distance between query and proposals to supervise model learning. Negative proposals can be the misaligned proposals within the same video (intra-video), or proposals from other videos (inter-video). Thus, MCN builds both intra and inter triple-based ranking loss (ref. Eqn. 8) as objectives. The intra loss differentiates subtle differences within a video, and inter loss differentiates broad semantic concepts. Based on MCN, Hendricks *et al.* [57] further propose MLLC, which treats video context as a latent variable and unifies MCN and CTRL for moment localization.

The prior methods encode the entire query into one feature vector, and apply simple cross-modal reasoning for feature fusion. However, treating queries holistically may obfuscate the keywords that have rich temporal and semantic cues. The simple fusion strategy also leads to inferior cross-modal understanding. Temporal dependencies and reasoning between video events and texts are not fully considered. Also, spatial-temporal information inside the video or query is overlooked. A number of methods are proposed to address these issues. Among them, ROLE [11], MCF [44], ACRN [12], TCMN [71], and ASST [72] mainly focus on refining the multimodal interaction/fusion between visual and textual features, through more sophisticated structures or semantic decomposition of video/query. ACL [13], built upon CTRL, explicitly mines activity concepts from both video and language modalities as prior knowledge, to calibrate the confidence of proposal to be the target moment. In addition to multimodal interaction refinement, SLTA [73] and MMRG [74] also exploit to incorporate appearance knowledge, *i.e.*, object-level spatial visual features, to enhance cross-modal reasoning as an additional view of video content. Instead of generating proposals at initial stage, Ning *et al.* [75] equip SW strategy inside their model enabling end-to-end training.

In general, early SW-based methods have simple architectures. These methods lack both in-depth analysis of semantic knowledge of modalities and fine-grained multimodal fusion mechanism, leading to inferior performance. The following up work attempts to address these weaknesses by devising various techniques to better exploit video content and query, enhancing cross-modal reasoning between them. Despite the continuous improvements, the two-stage sliding window-based methods suffer from inevitable



(a) Query-guided segment proposal network.



(b) The early fusion retrieval model of QSPN.

Fig. 12. QSPN architecture, reproduced from Xu *et al.* [45].

drawbacks. Specifically, densely sampling proposals with multi-scale sliding windows results in heavily computational cost, as many overlapped areas are re-computed. These methods are also sensitive to negative samples, where fallacious negative samples may lead to inferior results.

4.1.2 Proposal Generated Method

Proposal generated (PG) method alleviates the computation burden of SW-based methods by avoiding the dense sampling process. Instead, PG methods generate proposals conditioned on the query. The number of proposals hence reduces remarkably.

Early proposal generated methods still follow the two-stage propose-and-rank pipeline. Xu *et al.* [14] employ a pre-trained segment proposal network (SPN) for proposal candidate generation, rather than adopting sliding windows. Based on Xu *et al.* [14], QSPN [45] further ameliorates SPN to produce query-specific proposal candidates. As illustrated in Fig. 12(a), QSPN interacts query embedding with visual features to derive temporal attention weights, and re-weights the visual features to refine proposal generation. With the generated proposal feature, QSPN sequentially encodes proposal with each token in query, and predicts the similarity score at last, shown in Fig. 12(b). QSPN is optimized by triple-based ranking loss (ref. Eqn. 8), while a captioning loss is adopted to improve performance via query regeneration. Similarly, SAP [46] directly trains a visual concept detector to generate proposal candidates by measuring visual-semantic correlations between query and video frames.

Although the two-stage PG methods mitigate computation complexity to some degree, they still encounter some ineluctable drawbacks. To achieve good performance, PG methods still need to sample proposal candidates relatively densely, to increase the chance that at least one proposal can cover or is close to ground-truth moment. Similar to SW-based methods, the two-stage PG methods also rely on ranking-based objectives, making them sensitive to negative samples. Besides, proposal candidates are processed separately; hence individual pairwise proposal-query matching may neglect the contextual information.

To overcome these defects, recent solutions [47], [48], [76] reformulate the pipeline of PG methods to a single-pass pattern, in an end-to-end manner. Specifically, BpNet [47] (see Fig. 13) and APGN [48] propose to replace the separate proposal generator by a proposal-free module (detailed in Section 4.2) and jointly train it

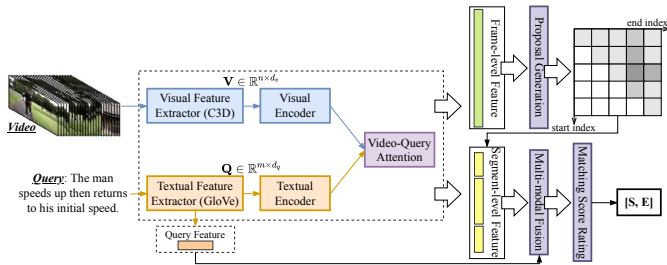


Fig. 13. BPNet architecture, reproduced from Xiao *et al.* [47].

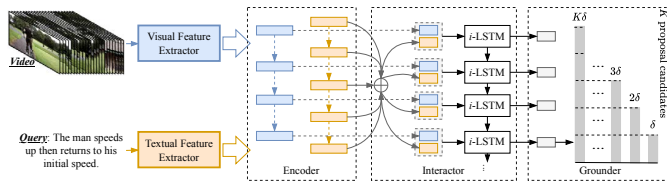


Fig. 14. TGN architecture, reproduced from Chen *et al.* [15].

with the main model. In this case, the proposal generation module is supervised by ground-truth moment, and only a few proposals are required to be generated. Besides, since the whole video is encoded as a feature sequence (ref. Section 2.3), visual features are jointly learned and interacted with query. Thus, the model is able to consider contextual information. LPNet [76] maintains a boundary-aware predictor and a learnable proposal module in parallel, where the boundary-aware predictor could refine predictions of the learnable proposal module. Furthermore, CMHN [77] generates proposal candidates with 1D regular convolution, and modeling proposal-query matching in the Hamming space through cross-modal hashing.

4.1.3 Anchor-based Method

Sliding window and the early proposal generated methods follow the two-stage propose-and-rank pipeline which suffers from various drawbacks. Researchers then source for alternative structures without pre-cutting proposal candidates at the input stage. One kind of solutions is anchor-based methods, which incorporate proposal generation into answer prediction and maintain the proposals with various learning modules. According to how the anchors are produced and maintained, we further classify them into standard anchor-based and 2D-Map methods.

Standard Anchor-based Method. Methods in this category produce proposal candidates with multi-scale anchors and maintain them sequentially or hierarchically in the model. They aggregate contextual multimodal information and generate the final grounding result in one pass. The first anchor-based method for TSGV is Temporal GroundNet (TGN) by Chen *et al.* [15], shown in Fig. 14. TGN temporally captures the evolving fine-grained frame-by-word interactions between video and query. At each time step, multi-scale proposal candidates ending at the current time are generated using pre-set anchors. Then a sequential LSTM grounder simultaneously scores the group of proposals. TGN adopts weighted binary cross-entropy loss (ref. Eqn. 9) to optimize the model. In contrast, MAN [16] and SCDM [17], [51] adopt temporal convolutional network to produce proposal candidates hierarchically. That is, proposals with different scales are generated at different levels of the stacked temporal convolution module.

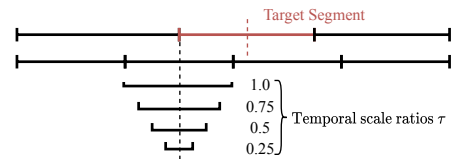


Fig. 15. Anchor scale in SCDM, reproduced from Yuan *et al.* [17].

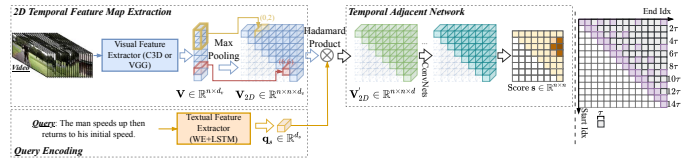


Fig. 16. 2D-TAN architecture, reproduced from Zhang *et al.* [18].

SCDM also adopts different multi-scale anchors compared to the standard version. As shown in Fig. 15, SCDM imposes different scale anchors based on a basic span centered at each time step.

Subsequent work generally follows the strategies of TGN or SCDM with more sophisticated learning modules and/or auxiliary objectives. To be specific, CMIN [50], [78], CBP [79], FIAN [80], HDRR [81], and MIGCN [82] adopt the strategy of TGN, while CSMGAN [83], RMN [84], IA-Net [85], and DCT-Net [86] apply the strategy of SCDM. These solutions design various cross-modal reasoning strategies to perform more fine-grained and deeper multi-modal interaction between video and query, for precise moment localization. In addition, CBP [79] introduces auxiliary boundary module to compute confidence of feature at each time step to be the boundary of target moment. Some other work adopt boundary regression module to refine the start and end time points of generated moments. MIGCN [82] develops a rank module apart from boundary regression module to distinguish the optimal proposal from a set of similar proposal candidates.

2D-Map Anchor-based Method. Standard anchor-based method produces proposal candidates with preset multi-scale anchors and maintains them sequentially or hierarchically. These proposals are individually processed and their temporal dependencies are not well considered. Further, lengths of proposals are restricted by preset anchors. 2D-Map methods use a two-dimensional map to model temporal relations between proposal candidates, shown in Fig. 5(d). Theoretically, 2D-Map could enumerate all possible proposals in any length, while maintaining their adjacent relations.

Before 2D-Map methods, a prior work TMN [87] first proposes to enumerate all possible consecutive segments as proposals and predict the best matched proposal as result through interacting each proposal with query. However, TMN generates proposals in the answer predictor; its enumeration strategy is more like a variant of standard anchor-based strategy.

2D-TAN [18] is the first solution modeling proposals with a 2D temporal map, and its overall architecture is shown in Fig. 16 left. 2D-TAN first extracts visual features and converts them into 2D feature map, while the query is encoded in sentence level representation. A temporal adjacent network is proposed to fuse the query feature with each proposal feature and embed the video context information with convolutional network. As shown in Fig. 16 right, 2D-TAN divides video into evenly spaced video snippets with duration τ , where (i, j) on the 2D map denotes a

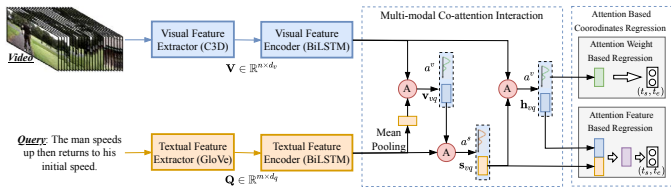


Fig. 17. ABLR architecture, reproduced from Yuan *et al.* [19].

proposal candidate from time $i\tau$ to $j\tau^4$. Instead of enumerating all possible consecutive segments as proposals, 2D-MAN proposes a sparse sampling strategy to remove redundant moments which have large overlaps with the selected proposals. The model adopts binary cross entropy loss for model learning. 2D-TAN is further extended [88] with multi-scale modeling to achieve a larger receptive field and obtain richer context. The extended version reduces the complexity of proposal generation from quadratic to linear, making the dense video prediction more efficient.

Due to its effectiveness, a series of work follows 2D-TAN’s proposal generation⁵ or its overall structure. As illustrated in Fig. 16, 2D-TAN directly encodes query into sentence-level representation and interacts with proposals via simple Hadamard product. In this sense, multimodal interaction is overlooked. To remedy, PLN [89], SMIN [53], CLEAR [90], and STCM-Net [91] disentangle video proposals into different temporal granularities [89], [91] or different semantic contents [53], [90], and perform cross-modal reasoning at both coarse- and fine-grained granularities. VLG-Net [92] and RaNet [54] maintain query words and video proposals in a graph, and adopt GCN [4], [93] to conduct intra- and inter-modal interactions for cross-modal reasoning. SV-VMR [94] decomposes query into multiple semantic roles [95] and performs multi-level cross-modal reasoning at semantic level. MATN [52] further concatenates proposals and query words into a sequence, and encodes them through a single-stream transformer network. It also devises a novel multi-stage boundary regression to refine the predicted moments. Instead of using the simple Hadamard product, DMN [96] proposes to project proposals and query features to common embedding space and leverage metric learning for cross-modal pair discrimination. Moreover, FVMR [55] claims that the standard cross-modal interaction module is inefficient and replaces it with a semantic embedding module to model multimodal interaction.

4.2 Proposal-free Method

Proposal-based methods perform various proposal generations, and essentially depend on the ranking of proposal candidates. In contrast, proposal-free methods directly predict the start and end boundaries of the target moment on fine-grained video snippet sequence, without ranking a vast of proposal candidates. Depending on the format of moment boundaries, proposal-free methods are categorized in to regression-based and span-based methods.

4.2.1 Regression-based Method

Regression-based method computes a time pair (t_s, t_e) and compares the computed pair with ground-truth (τ_s, τ_e) for model optimization. Attention-based location regression (ABLR) [19] is

4. $i \leq j$, *i.e.*, only the upper triangular area of 2D map is valid

5. Some methods follow 2D-TAN’s proposal generation to produce proposal candidates, but they may not maintain the proposals with 2D map.

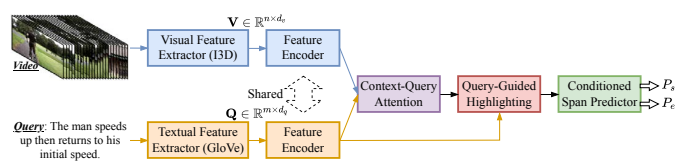


Fig. 18. VSLNet architecture, reproduced from Zhang *et al.* [23].

one of the first regression-based solutions for TSGV. Depicted in Fig. 17, ABLR extracts visual and textual features and encodes them through BiLSTM networks to aggregate contextual information, respectively. Then, a three-stage multimodal co-attention is developed to perform cross-modal reasoning. The multimodal feature is fed to regressor for moment prediction. ABLR explores two types of regressor. One is attention weight-based regression, which takes video attention weights as inputs. Another is attended feature based regression, which fuses the attended visual and textual features as inputs. The model is optimized by smoothed L_1 loss. ABLR also devises an attention calibration loss to refine video attentions, which encourages higher attention weights to video snippets within the ground-truth moment.

Concurrently, ExCL [20] also addresses TSGV by regression and designs three different answer predictors following ideas from reading comprehension in NLP [6]–[8]. Similar to proposal-based methods, subsequent regression work [22], [97]–[103] dives in designing various feature encoding and cross-modal reasoning strategies for superior multimodal interaction and accurate moment localization. From the perspective of regression, DEBUG [22], GDP [97], and DRN [99] analyze data imbalance issue in TSGV: the number of video frames is large, but the positive samples are sparse *i.e.*, only two frames for start and end timestamps. They regard all frames within ground-truth moment as positive, and densely predict the distances to boundaries for each frame within ground-truth moment to mitigate the sparsity issue. CMA [98] and DeNet [102] study bias issue in TSGV. Specifically, CMA [98] rectifies the inevitable annotation bias by moment boundary ambiguities via two-branch cross-modality attention network and a task-specific regression loss. DeNet [102] disentangles query into relation and modified features, and devises a debias mechanism to alleviate both query uncertainty and annotation bias issues. Bias issues will be further discussed in Section 6.1.

There are also regression-based methods [104]–[106] incorporating additional modalities from video to improve localization performance. For instance, HVTG [104] extracts both appearance and motion, PMI [105] further exploits audio features from video extracted by SoundNet [107]. DRFT [106] leverages visual, optical flow, and depth flow features of video, and analyzes retrieval results of different feature view combinations.

4.2.2 Span-based Method

Span-based methods aim to predict the probability of each video snippet/frame being the start and end positions of target moment. Inspired by reading comprehension (RC) task in NLP [6]–[8], L-Net [21] and ExCL [20] first formulate TSGV as a span prediction task. In addition to the regression-based predictors, ExCL also designs corresponding span prediction heads.

Based on these two work, Zhang *et al.* [23] further compare differences between RC and TSGV tasks, and propose VSLNet. Specifically, video is continuous and causal relations

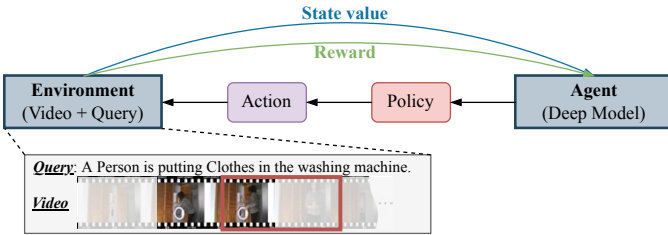


Fig. 19. Illustration of sequence decision making formulation in TSGV.

between video events are usually adjacent, while words in query are discrete and demonstrate syntactic structure. Shown in Fig. 18, VSLNet exploits a context-query attention modified from QANet [7] to perform fine-grained multimodal interaction. Then a conditioned span predictor computes the probabilities of start/end boundaries of target moment. VSLNet also introduces a query-guided highlighting module to bridge the gaps between RC and TSGV. This module effectively narrows down moment search space to a smaller highlighted region. Existing methods including VSLNet generally perform better on short videos than long videos. Their follow up work [65] extends VSLNet to handle long videos by incorporating the concepts from multi-paragraph question answering [108]. Long videos are split into multiple short videos and a hierarchical searching strategy is deployed for moment localization.

In general, overall frameworks of regression- and span-based methods are similar. Thus, the continuous performance improvements of subsequent work [109]–[121] are also achieved by modifying the feature encoding and multimodal interaction modules, introducing auxiliary objectives, and/or augmenting additional features. In particular, SeqPAN [110] introduces the concepts of named entity recognition [122]–[124] in NLP by splitting snippet sequence into begin, inside, and end regions of target moment, and background region. IVG-DCL [112] introduces dual contrastive learning mechanism to enhance multimodal interaction and leverages structured causal model [125] to address the selection bias of TSGV. CI-MHA [114] proposes to remedy the start/end prediction noise caused by annotator disagreement via an auxiliary moment segmentation task. ABIN [117] devises an auxiliary adversarial discriminator networks to produce coordinate and frame correlation distributions for moment boundary refinement. DORi [119] incorporates appearance features and captures the relations between objects and actions guided by query. CBLN [120] addresses TSGV from a new perspective. It reformulates TSGV by scoring all pairs of start and end indices simultaneously and predict moment with a biaffine structure.

4.3 Reinforcement Learning-based Method

From the perspective of proposal usage, reinforcement learning (RL) based methods are also proposal-free methods. However, task formulation of RL-based method is fundamentally different from the proposal-free methods reviewed earlier. RL-based method formulates TSGV as a sequence decision making problem, and utilizes deep reinforcement learning techniques to solve it.

Illustrated in Fig. 19, RL-based method usually maintains a sliding window (the dark red rectangle). The sliding window here is different from that discussed in Section 4.1. RL-based method only adopts a single window, controlled by an agent. An agent, *i.e.*, a learnable module, controls the movement of the window based

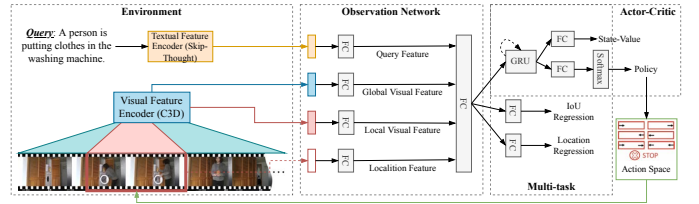


Fig. 20. RWM-RL architecture, reproduced from He *et al.* [24].

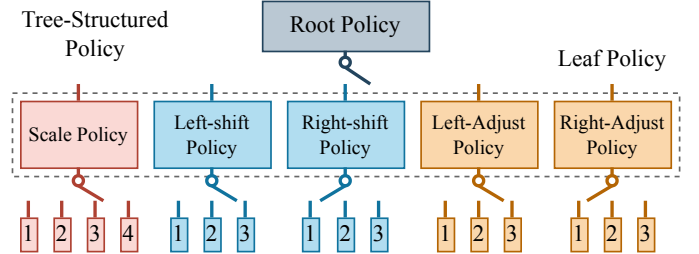


Fig. 21. Tree-structured policy, reproduced from Wu *et al.* [26].

on a set of handcraft-designed temporal transformations, *e.g.*, shifting and scaling. At each learning step, after each movement, a reward is generated to indicate whether the window is closer or farther away from the target moment. The agent will adapt its action for next step within the pre-defined action space.

RWM-RL [24] is one of the first work to define and solve TSGV with a RL framework. Shown in Fig. 20, RWM-RL consists of three modules. The environment module converts the query, global video, and local video segment within the window into corresponding representations. Then the observation network fuses the query and video features to output the current state of the environment, *i.e.*, multimodal representation, at each learning step. In the decision making module (*i.e.*, agent), RWM-RL leverages the actor-critic algorithm [126] to compute the state-value and an action policy, *i.e.*, the probabilistic distribution of all pre-designed actions in the action space. The state-value is used for reward computation, and the action policy determines the movement of sliding window to adjust the temporal boundaries. RWM-RL defines 7 actions: moving start/end point ahead/backward by δ (4 scaling actions), shifting both start and end point backward/forward by δ (2 shifting actions), and a STOP action, where δ denote a basic moving distance. In general, the iterative process ends when encountering the STOP action or reaching the preset maximum number of iteration steps. RWM-RL adopts GRU to model the sequential decision making process for actor-critic module. A reward is computed at each step, where the reward is designed to encourage the agent to find a better matching position step by step. All the rewards are accumulated for model optimization by utilizing the advantage function [126] as objective and Monte Carlo sampling [127] for policy gradient approximation. To increase action diversity, RWM-RL further introduces entropy of the policy output as an auxiliary objective following A2-RL [128].

SM-RL [25] presents a RNN-based semantic matching RL model to selectively observe proposal candidates produced by a controllable agent. TSP-PRL [26] designs a hierarchical action space with tree-structured policy, inspired from human’s coarse-to-fine decision making mechanism. The action selection is controlled by a switch over an interface in tree-structured policy (see Fig. 21). AVMR [129] treats RL-based module as a generator,

and devises a Bayesian ranking module as discriminator to rank proposals. STRONG [130] considers both appearance and motion features, and employs parallel spatial-level and temporal-level RL modules for moment localization. TripNet [131] mainly focuses on ameliorating the observation network to boost performance. Instead of using sliding windows, MABAN [132] leverages two individual agents to model start and end points separately. The two agents are conditioned on each other to avoid invalid predictions.

4.4 Other Supervised Method

In addition to the aforementioned method categories, researchers also explore other types of formulation to address TSGV, or under different settings. Shao *et al.* [133] design a unified framework based on TAG [134] to perform both video-level retrieval and moment-level localization simultaneously. The two tasks could reinforce each other. DPIN [135] devises a dual-path interaction network to integrate the benefits of both proposal-based and proposal-free methods. Inspired by Patrick *et al.* [136], Ding *et al.* [137] propose a support-set based cross-supervision strategy to enhance multimodal interaction learning, through discriminative contrastive and generative caption objectives. Bao *et al.* [138] claim that multiple moments in a video are semantically correlated and temporally coordinated according to their order. Thus, they explore a novel setting of TSGV, dubbed as dense events grounding. This setting allows jointly localizes multiple moments described in a paragraph, *i.e.*, multiple sentences. SNEAK [139] studies adversarial robustness of TSGV models by examining three facets of vulnerabilities, *i.e.*, vision, language, and cross-modal interaction, from both attack and defense aspects. Xu *et al.* [140] further investigate model pre-training for TSGV by constructing a large-scale synthesized dataset with annotations, and designing a novel boundary-sensitive pretext task. Cao *et al.* [141] reformulate TSGV as a set prediction task, and propose a multimodal transformer model inherited from DETR [142].

4.5 Summary of Supervised Method

Hereto we have reviewed different categories of supervised TSGV methods, as well as their advantages and shortcomings. In general, early sliding window-based and proposal generated methods suffer from low efficiency and flexibility, because of dense and overlapped proposals. These methods also rely on ranking-based loss, making them sensitive to negative samples. Anchor-based methods, another form of proposal-based solution, learn TSGV in an end-to-end manner. The proposal generation process is incorporated into the model, abnegating the ineffective SW and PG strategies. Anchor-based methods also enable contextualized representation learning and fine-grained multimodal interaction. However, the anchor-based methods still need to maintain a mass of proposals during prediction, which hinders model efficiency.

Proposal-free methods directly learn to predict the boundaries of target moment, without maintaining any proposals. These methods are more efficient and are flexible to adapt to moments with diverse lengths. Nevertheless, compared to proposal-based methods, proposal-free methods overlook the rich information between start and end boundaries and fail to exploit the proposal-level interaction. They also suffer from severe imbalance issue between the positive and negative training samples, *i.e.*, only two (start and end) frames are positive in the whole video. Also belonging to proposal-free category, the design of RL-based methods is intuitive and effective, kind of simulating human’s

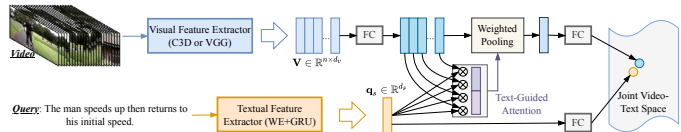


Fig. 22. TGA architecture, reproduced from Mithun *et al.* [27].

decision making strategy. However, their performance is unstable due to the difficulty of optimizing RL-based methods.

Despite vast number of methods in each category, all methods focus on ameliorating the cross-modal reasoning module, to achieve fine-grained and precise multimodal interaction. That also means that the high-level pipeline of methods in each category is similar in general. Recall that feature interactor is responsible for understanding the semantic concepts of both query and video, and fusing them to emphasize the video contents that are semantically relevant to query. In this sense, quality of interactor module determines a TSGV model’s performance to a great extent.

4.6 Weakly-supervised TSGV Method

Supervised learning usually needs a large number of annotations for model training. Annotating temporal boundaries on video with text description is extremely time-consuming and labor-intensive, often not scalable. Further, annotations also suffer from inaccurate issue, *i.e.*, action boundaries in videos are usually subjective and inconsistent across different annotators.

Under weakly-supervised setting, TSGV methods only need video-query pairs but not the annotations of starting/end time. They explore to find results in a shared multimodal feature space or with reconstruction-based strategy. In general, existing weakly-supervised TSGV methods can be roughly grouped into multi-instance learning and reconstruction-based models.

4.6.1 Multi-Instance Learning Method

Multi-instance learning method generally regards the input video as bag of instances with bag-level annotations. The prediction of instance, *i.e.*, proposal candidates, is aggregated as bag-level prediction.

TGA [27] first solves TSGV under the multi-instance learning setting. As shown in Fig. 22, TGA first encodes video and query features, and presents a text-guided attention to learn text-specific global video representations. Then both visual and textual features are projected to a joint space. TGA regards the video and its corresponding query descriptions as positive pairs, while the video with other queries and the query with other videos as negative pairs. TGA learns visual-text alignment at the video-level by maximizing matching scores of positive samples while minimizing scores of negative samples.

To achieve good performance, MIL-based methods have to perform precise semantics alignment between video and query. Thus, subsequent solutions [28], [143]–[154] mainly focus on devising sophisticated cross-modal alignment module, designing robust proposal selection strategy, and/or building effective learning objectives. WSLLN [28] models alignment and detection modules in parallel to perform proposal selection and video-level alignment simultaneously. VLANet [144] designs surrogate proposal selection module to prune irrelevant proposal candidates. Chen *et al.* [143] and Teng *et al.* [152] perform video-query alignment at multiple granularities. CCL [146] and VCA [148] introduce

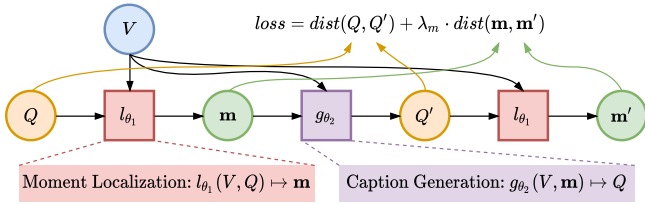


Fig. 23. WS-DEC architecture, reproduced from Duan *et al.* [29].

contrastive learning mechanism to effectively distinguish positive and negative (or counterfactual positive) proposals. BAR [145] involves additional RL module to progressively refine retrieved proposals. FSAN [149], WSTAN [153], and LoGAN [154] focus on mining video and query contents and their correlations. Then they design fine-grained cross-modal alignment module for accurate moment localization. Da *et al.* [147] study the uncertain across-positive frame issue, *i.e.*, an object might appear sparsely across multiple frames, and devise a AsyNCE loss to mitigate the issue by disentangling positive pairs from negative ones. CRM [150] uses a cross-sentence relation mining strategy to explicitly model cross-sentence relations in paragraph and explore cross-moment relations in video. LCNet [151] further deploys self-supervised cycle consistent loss to guide video-query matching.

4.6.2 Reconstruction-based Method

Reconstruction-based method tackles TSGV in an indirect way. Methods in this category first take video and query as inputs to produce desired proposals matched to the query. Then the proposals are used to reconstruct the query, where the intermediate proposals are treated as localization results.

The idea of reconstruction is first explored by Duan *et al.* [29]. They propose a method to solve weakly supervised dense event captioning (WS-DEC), where moment localization is an auxiliary sub-task to assist model training. The authors indicate that moment localization and event captioning are a pair of dual tasks. Moment localization is to learn a mapping $l_{\theta_1} : (V, Q) \mapsto \mathbf{m}$, *i.e.*, retrieving a moment \mathbf{m} corresponded to the caption C_i from video V . Event captioning inversely generates caption Q for the given \mathbf{m} , *i.e.*, $g_{\theta_2} : (V, \mathbf{m}) \mapsto Q$. Since Q and \mathbf{m} is an one-to-one correspondence, the dual problems exist simultaneously, and Q and \mathbf{m} are tied together. By nesting the dual functions, caption-moment pair (Q, \mathbf{m}) becomes a fixed-point solution as:

$$Q = g_{\theta_2}(V, l_{\theta_1}(V, Q)), \quad \mathbf{m} = l_{\theta_1}(V, g_{\theta_2}(V, \mathbf{m})), \quad (16)$$

where l_{θ_1} and g_{θ_2} are the localization and captioning modules, respectively. As shown in Fig. 23, WS-DEC first retrieves moment \mathbf{m} by giving video V and caption Q ; Then the retrieved \mathbf{m} and V are used to reconstruct the caption, denoted by Q' ; Finally, the reconstructed Q' and V are utilized to relocate the moment \mathbf{m}' again. The objective of WS-DEC is to minimize the distances of $\mathbf{m}-\mathbf{m}'$ and $Q-Q'$ pairs simultaneously.

SCN [30] adopts a similar idea as WS-DEC. However, SCN is designed for solving weakly supervised TSGV directly; it does not use a specific caption generation module, but switches to reconstruct the masked query. As depicted in Fig. 24, SCN first retrieves a set of proposals from video. The model then selects top- K proposals as inputs to reconstruct masked query, and compute rewards based on reconstruction loss. The rewards further act as feedback to refine proposal generation. MARN [155] leverages

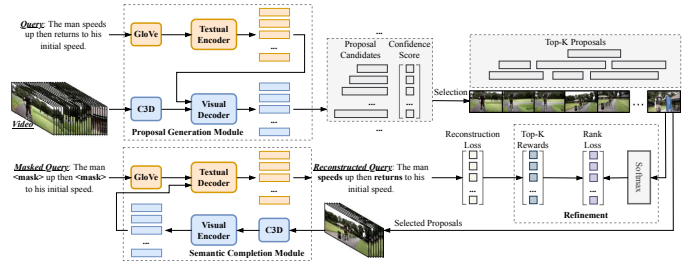


Fig. 24. SCN architecture, reproduced from Lin *et al.* [30].

both proposal-level and clip-level video features to produce more accurate proposal candidates. The proposal-level and clip-level features are generated by 2D-Map strategy [18] and BMN [156], respectively. EC-SL [31], [157] improves WS-DEC by introducing a concept learner and an induced set attention block.

4.6.3 Other Weakly-supervised Method

In addition to MIL and reconstruction-based methods, Zhang *et al.* [158] consider both inter- and intra-sample confrontments to address the drawback of standard MIL-based methods. The latter generally ignores intra-sample confrontation between moments with semantically similar contents. Luo *et al.* [159] present a new setting of TSGV task, also in a semi-supervised way. They construct a teacher-student network. The teacher module produces instant pseudo labels for unlabeled samples based on predictions. The student module learns from pseudo labels via self-supervised learning. Nam *et al.* [160] further propose to learn a TSGV model in zero-shot manner to eliminate annotation cost. In zero-shot setting, video-query pairs are not provided. They utilize off-the-shelf object detector and pseudo-query generation module fine-tuned on RoBERTa [38] to produce proposals and queries, and simulate the standard TSGV learning. Gao *et al.* [161] also explore to leverage off-the-shelf visual concept detector and a pre-trained image-sentence embedding space to perform TSGV without using text annotations on video.

5 PERFORMANCE COMPARISON

Performance Overview. We now summarize the reported performance on benchmark datasets. Table 2 summarizes the consecutive improvements of supervised TSGV methods over years, by category, on Charades-STA, ActivityNet Captions, and TACoS datasets. In general, anchor-based (ANchor and 2D-map) and proposal-free (ReGression and SpaN) methods are superior to sliding window-based (SW) and proposal generated (PG) methods. Within the SW category, recent model MMRG [74] introduces graph structure to model the visual-textual relations, and adds boundary regression auxiliary objective to guide moment retrieval, outperforming early SW methods by a large margin. Similar observation holds in PG category. Compared to early anchor-based and proposal-free work, recent methods incorporate more sophisticated multimodal interaction strategies to refine the cross-modal reasoning between video and query. They also introduce various auxiliary objectives to enhance the feature representation learning and steer the model for more precise moment localization. In RL category, recent solutions mainly focus on designing more powerful agents or refined action space (policy) to achieve accurate sequence decisions [26], [132]. Despite the improvements

TABLE 2

R@1, IoU=m of supervised methods. SW: Sliding Window-based, PG: Proposal Generated, AN: standard Anchor-based, 2D: 2D-Map, RG: Regression-based, SN: Span-based, RL: Reinforcement Learning-based methods.

Category	Method	Venue	Charades-STA			ActivityNet Captions			TACoS _{org}			TACoS _{2DTAN}		
			m=0.3	m=0.5	m=0.7	m=0.3	m=0.5	m=0.7	m=0.3	m=0.5	m=0.7	m=0.3	m=0.5	m=0.7
SW	CTRL [9]	ICCV'17	-	23.63	8.89	-	-	-	18.32	13.30	-	-	-	-
	ROLE [11]	ACM MM'18	25.26	12.12	-	-	-	-	-	-	-	-	-	-
	ACRN [12]	SIGIR'18	-	-	-	-	-	-	19.52	14.62	-	-	-	-
	SLTA [73]	ICMR'19	38.96	22.81	8.25	-	-	-	17.07	11.92	-	-	-	-
	ACL-K [13]	WACV'19	30.48	12.20	-	-	-	-	24.17	20.01	-	-	-	-
	MMRG [74]	CVPR'21	71.60	44.25	-	-	-	-	-	-	-	57.83	39.28	-
PG	QSPN [45]	AAAI'19	54.70	35.60	15.80	45.30	27.70	13.60	-	-	-	-	-	-
	SAP [46]	AAAI'19	-	27.42	13.36	-	-	-	-	18.24	-	-	-	-
	BPNet [47]	AAAI'21	65.48	50.75	31.64	58.98	42.07	24.69	25.96	20.96	14.08	-	-	-
	APGN [48]	EMNLP'21	-	62.58	38.86	-	48.92	28.64	-	-	-	40.47	27.86	-
AN	TGN [15]	EMNLP'18	-	-	-	45.51	28.47	-	21.77	18.90	-	-	-	-
	CMin [50]	SIGIR'19	-	-	-	63.61	43.40	23.88	24.64	18.05	-	-	-	-
	SCDM [17]	NeurIPS'19	-	54.44	33.43	54.80	36.75	19.86	26.11	21.17	-	-	-	-
	CBP [79]	AAAI'20	-	36.80	18.87	54.30	35.76	17.80	27.31	24.79	19.10	-	-	-
	FIAN [80]	ACM MM'20	-	58.55	37.72	64.10	47.90	29.81	33.87*	28.58*	-	-	-	-
	IA-Net [85]	EMNLP'21	-	61.29	37.91	67.14	48.57	27.95	-	-	-	37.91	26.27	-
2D	2D-TAN [18]	AAAI'20	-	39.81	23.31	59.45	44.51	27.38	-	-	-	37.29	25.32	-
	MATN [52]	CVPR'21	-	-	-	-	48.02	31.78	-	-	-	48.79	37.57	-
	SMin [53]	CVPR'21	-	64.06	40.75	-	48.46	30.34	-	-	-	48.01	35.24	-
	RaNet [54]	EMNLP'21	-	60.40	39.65	-	45.59	28.67	-	-	-	43.34	33.54	-
	FVMR [55]	ICCV'21	-	55.01	33.74	60.63	45.00	26.85	-	-	-	41.48	29.12	-
	CLEAR [90]	TIP'21	-	-	-	59.96	45.33	28.05	-	-	-	42.18	30.27	15.54
RG	ABLR [19]	AAAI'19	-	-	-	55.67	36.79	-	19.50	9.40	-	-	-	-
	ExCL [20]	NAACL'19	61.50	44.10	22.40	63.00	43.60	24.10	45.50	28.00	13.80	-	-	-
	DEBUG [22]	EMNLP'19	54.95	37.39	17.92	55.91	39.72	-	23.45	-	-	-	-	-
	DRN [99]	CVPR'20	-	53.09	31.75	-	45.45	24.36	-	23.17	-	-	-	-
	LGI [100]	CVPR'20	72.96	59.46	35.48	58.52	41.51	23.07	-	-	-	-	-	-
	CPNet [101]	AAAI'21	-	60.27	38.74	-	40.56	21.63	-	-	-	42.61	28.29	-
SN	VSLNet [23]	ACL'20	70.46	54.19	35.22	63.16	43.22	26.16	29.61	24.27	20.03	-	-	-
	CPN [111]	CVPR'21	75.53	59.77	36.67	62.81	45.10	28.10	-	-	-	48.29	36.58	21.58
	CI-MHA [114]	SIGIR'21	69.87	54.68	35.27	61.49	43.97	25.13	-	-	-	-	-	-
	SeqPAN [110]	ACL'21	73.84	60.86	41.34	61.65	45.50	28.37	31.72	27.19	21.65	48.64	39.64	28.07
	ACRM [116]	TMM'21	73.47	57.93	38.33	-	-	-	-	-	-	51.26	39.34	26.94
	VSLNet-L [65]	TPAMI'21	70.46	54.19	35.22	62.35	43.86	27.51	32.04	27.92	23.28	47.66	36.34	26.42
RL	RWM-RL [24]	AAAI'19	-	36.70	-	-	36.90	-	-	-	-	-	-	-
	SM-RL [25]	CVPR'19	-	24.36	11.17	-	-	-	20.25	15.95	-	-	-	-
	TSP-PRL [26]	AAAI'20	-	45.45	24.75	56.02	38.82	-	-	-	-	-	-	-
	TripNet [131]	BMVC'20	54.64	38.29	16.07	48.42	32.19	13.93	23.95	19.17	9.52	-	-	-
	MBAN [132]	TIP'21	-	56.29	32.26	-	42.42	24.34	-	-	-	-	-	-
Other	DPIN [135]	ACM MM'20	-	47.98	26.96	62.40	47.27	28.31	-	-	-	46.74	32.92	-
	GTR [141]	EMNLP'21	-	62.58	39.68	-	50.57	29.11	-	-	-	40.39	30.22	-
	BSP [140]	ICCV'21	68.76	53.63	29.27	-	-	-	-	-	-	-	-	-

TABLE 3
Results of supervised methods on DiDeMo dataset.

Category	Method	Venue	R@1, IoU=m			mIoU
			0.5	0.7	1.0	
SW	MCN [10]	ICCV'17	-	-	28.10	41.08
	MLLC [57]	EMNLP'18	-	-	27.46	41.20
	ROLE [11]	ACM MM'18	29.40	15.68	-	-
	ACRN [12]	SIGIR'18	27.44	16.65	-	-
	SLTA [73]	ICMR'19	30.92	17.16	-	-
AN	TGN [15]	EMNLP'18	-	-	28.23	42.97
	MAN [16]	CVPR'19	-	-	27.02	41.16
2D	VLG-Net [92]	ICCV'21	33.35	25.57	25.57	-
RL	SM-RL [25]	CVPR'19	-	-	31.06	43.94

distinct. Two possible reasons for the inferior results are: (i) RL learning process is not very stable, and (ii) the multimodal interaction between two modalities is not fully exploited in RL methods. Among other methods, GTR [141] and BSP [140] provide new perspective to solve TSGV. BSP proposes a pre-training paradigm for TSGV by designing a boundary-sensitive pretext task and collecting a synthesized dataset with temporal boundaries. GTR builds an end-to-end framework to learn TSGV from raw videos directly. Although their results are slightly inferior to other solutions, both open up new directions for TSGV. Results of DiDeMo dataset are reported in Table 3. As videos in DiDeMo are pre-segmented into fixed-length clips, this dataset is less suitable for proposal-free methods.

of recent RL-based methods, the performance gap between RL-based methods and anchor-based/proposal-free methods remains

Table 4 reports results of some weakly-supervised methods on Charades-STA, ActivityNet Captions, and DiDeMo. TACoS is seldom used in weakly-supervised methods. In general, MIL-

TABLE 4

Results of weakly-supervised methods, where MIL is Multi-Instance Learning-based method, REC denotes Reconstruction-based method, and * denotes the zero-shot setting.

Category	Method	Venue	Charades-STA R@1, IoU= m			ActivityNet Captions R@1, IoU= m				DiDeMo R@ n , IoU=1.0		
			$m=0.3$	$m=0.5$	$m=0.7$	$m=0.1$	$m=0.3$	$m=0.5$	$m=0.7$	$n=1$	$n=5$	mIoU
MIL	TGA [27]	CVPR'19	32.14	19.94	8.84	-	-	-	-	12.19	39.74	24.92
	WSLLN [28]	EMNLP'19	-	-	-	75.40	42.80	22.70	-	19.40	54.40	27.40
	VLANet [144]	ECCV'20	45.24	31.83	14.17	-	-	-	-	19.32	65.68	25.33
	CCL [146]	NeurIPS'20	-	33.21	15.68	-	50.12	31.07	-	-	-	-
	LoGAN [154]	WACV'21	51.67	34.68	14.54	-	-	-	-	39.20	64.04	38.28
	VCA [148]	ACM MM'21	58.58	38.13	19.57	67.96	50.45	31.00	-	-	-	-
	FSAN [149]	EMNLP'21	-	-	-	78.45	55.11	29.43	-	19.40	57.85	31.92
	CRM [150]	ICCV'21	53.66	34.76	16.37	81.61	55.26	32.19	-	-	-	-
	LCNet [151]	TIP'21	59.60	39.19	18.87	78.58	48.49	26.33	-	-	-	-
	WSTAN [153]	TMM'21	43.39	29.35	12.28	79.78	52.45	30.01	-	19.40	54.64	31.94
REC	WS-DEC [29]	NeurIPS'18	-	-	-	62.71	41.98	23.34	-	-	-	-
	SCN [30]	AAAI'20	42.96	23.58	9.97	71.48	47.23	29.22	-	-	-	-
	MARN [155]	ArXiv'20	48.55	31.94	14.81	-	47.01	29.95	-	-	-	-
	EC-SL [31]	CVPR'21	-	-	-	68.48	44.29	24.16	-	-	-	-
Other	RTBPN [158]	ACM MM'20	60.04	32.36	13.24	73.73	49.77	29.63	-	20.79	60.26	29.81
	U-VMR [161]	TCSVT'21	46.69	20.14	8.27	69.63	46.15	26.38	11.64	-	-	-
	PSVL [160]*	ICCV'21	46.47	31.29	14.17	-	44.74	30.08	14.74	-	-	-

TABLE 5

Result of different visual features on Charades-STA.

Method	Category	Venue	Feature	R@1, IoU= m		
				$m=0.3$	$m=0.5$	$m=0.7$
DRN [99]	RG	CVPR'20	VGG	-	42.90	23.68
			C3D	-	45.40	26.40
			I3D	-	53.09	31.75
CPNet [101]	RG	AAAI'21	C3D	-	40.32	22.47
			I3D	-	60.27	38.74
BPNet [47]	PG	AAAI'21	C3D	55.46	38.25	20.51
			I3D	65.48	50.75	31.64
LPNet [76]	PG	EMNLP'21	C3D	59.14	40.94	21.13
			I3D	66.59	54.33	34.03
RaNet [54]	2D	EMNLP'21	VGG	-	43.87	26.83
			I3D	-	60.40	39.65

based methods are superior to reconstruction-based methods. Other than cross-modal reasoning, the learning objective also plays a key role in MIL-based methods. Recent solutions adopt more effective strategies or introduce auxiliary objectives, such as contrastive learning [146], pseudo supervision [28], [153], and boundary adjustment [143]. For other methods, PSVL [160] solves TSGV under the zero-shot setting. Zero-shot setting assumes that the video-query pairs are inaccessible, *i.e.*, only the text corpora and video collection are given. Although zero-shot setting is more challenging, arguably the setting is closer to real-world scenario.

Impact of Features. Improvements in model performance may come from various sources. In particular, various visual (*e.g.*, VGG [42], ResNet [162] C3D [1], I3D [3]) and textual (*e.g.*, GloVe [36], BERT [37]) feature extractors have been utilized in different models. Among visual feature extractors, VGG [42] and ResNet [162] are pre-trained on image datasets, and they are more effective in extracting appearance features like objects and visual concepts from video frames. In contrast, C3D [1] and I3D [3] are pre-trained on video action recognition datasets, for extracting motion features like actions or activities, from video snippets or segments. Summarized in Table 5, feature analysis

conducted by different methods on Charades-STA dataset shows that $VGG < C3D < I3D$, with respect to model performance. Because TSGV is mainly for activities retrieval, video-based feature extractors are more effective than image-based counterparts. I3D contains more sophisticated structure and is trained on larger datasets than C3D, leading to more powerful representation ability.

Visual features are mostly extracted from RGB frames. Chen *et al.* [106] explore to incorporate optical flow and depth maps information in frames as complementary visual features. Optical flow focuses on large motion, and depth maps reflects scene configuration when the action is related to objects recognizable with their shapes. Prominent improvements are obtained by adding more visual modality features on Charades-STA and ActivityNet Captions. A query may contain descriptions of both objects and actions. Thus, some methods [105], [119] exploit both appearance and motion features to represent a video. In addition to motion features extracted by C3D model, Chen *et al.* [105] introduce appearance features by IRV2 [162] and audio features from video by SoundNet [107]. In general, improving feature extractor or exploiting more diverse features leads to better accuracy.

6 CHALLENGES AND FUTURE DIRECTIONS

Despite performances made on benchmark datasets, limitations of TSGV methods and benchmarks hinder practicability and generalization ability of TSGV methods. Before we list future research directions, we review critical analysis on current methods and benchmarks.

6.1 Critical Analysis

Data Uncertainty. Recent studies [102], [163] observe that annotations among current benchmarks are ambiguous and inconsistent, *i.e.*, annotation uncertainty. Due to subjectivity, the annotated moment of a query may discrepant across annotators [163]. Zhou *et al.* [102] further point out query uncertainty, stemming from different expressions for a same moment. Although multiple queries with different expressions actually describe the same moment,

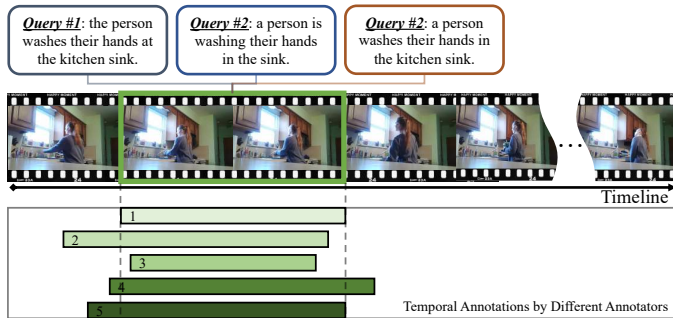


Fig. 25. Illustration of data uncertainty in TSGV benchmarks. Annotation uncertainty means disagreements of annotated ground-truth moment across different annotators. Query uncertainty means various query expressions for one ground-truth moment.

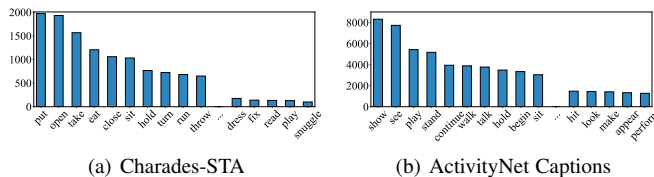


Fig. 26. The top-30 frequent actions in Charades-STA and ActivityNet Captions datasets.

TSGV models often generate quite different predictions. Fig. 25 depicts an example of annotation and query uncertainties.

To mitigate the annotation uncertainty, Otani *et al.* [163] re-annotate the benchmark datasets, resulting in multiple ground-truth moment for a query if exists. They also present two alternative evaluation metrics by considering multiple ground-truths. Zhou *et al.* [102] address both annotation and query uncertainties from the model design perspective. For query uncertainty, they decouple query into semantic phrases and modified tokens, and represent them separately. For annotation uncertainty, they propose a debias mechanism to generate diverse predictions. Nevertheless, the uncertainty issue remains far apart to be solved.

Data Bias. Otani *et al.* [163] and Yuan *et al.* [70] conduct analysis on Charades-STA and ActivityNet Captions, by counting frequent actions in queries and visualizing joint distributions of the start and end timestamps of ground-truth moment. As shown in Fig. 26, top-ranked action verbs cover most of the actions in the dataset *i.e.*, long-tail. A large number of queries describe some common events, while only a few queries covering the remaining actions. Fig. 27 shows that moment distributions are identical in train and test sets with distinct distributional bias for both datasets. Because of the distributional bias, a TSGV model could make a good guess of target moment, even without taking into consideration the input video and query [163].⁶ Yuan *et al.* [70] further re-organize the two datasets and develop Charades-CD and ActivityNet-CD datasets. Each dataset contains two versions of test sets, *i.e.*, the independent-and-identical distribution (iid) test set, and the out-of-distribution (ood) test set (see Fig. 28). Experiment results show that baselines generally achieve impressive performance on iid test set, but fail to generalize on ood test set.

To alleviate distributional bias, Yang *et al.* [164] develop a deconfounded cross-modal matching method to remove distribu-

6. Note weakly-supervised methods do not require annotated samples for training, thus they are naturally immune to the distributional bias.

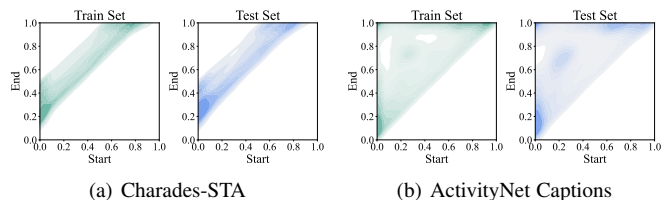


Fig. 27. An illustration of moment distributions for Charades-STA and ActivityNet Captions, where “Start” and “End” axes represent the normalized start and end timestamps, respectively. The deeper the color, the larger density (*i.e.*, more annotations) in the dataset.

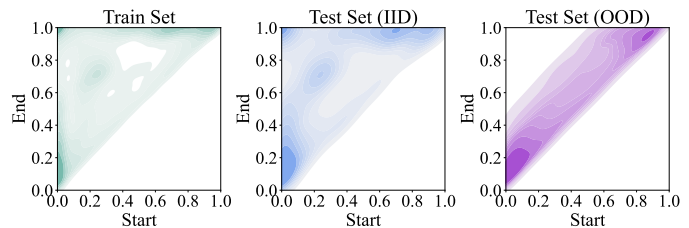


Fig. 28. Illustration of moment distributions of ActivityNet-CD dataset.

tional bias by leveraging the structured causal mechanism [125]. Luo *et al.* [159] devise a self-supervised method to solve TSGV with pseudo label generation. Zhang *et al.* [165] disentangles bias from TSGV model by adjusting losses to compensate for biases dynamically. Although solutions are developed to address moment distributional bias *e.g.*, debias strategies and dataset reorganization, it is unclear if current benchmarks provide the right setup to evaluate TSGV methods. Meanwhile, the long tail issue of action verb distribution in queries requires in-depth exploration and remains to be addressed.

Because of the inevitable limitations of current benchmark datasets, Soldan *et al.* [64] present the MAD dataset very recently. MAD comprises long-form videos, highly descriptive sentences, and large diversity in vocabulary. Most importantly, the timestamps of moments are uniformly distributed in the video. Lei *et al.* [166] also develop a new benchmark dataset termed QVHighlights to avert the data bias of existing TSGV datasets.

6.2 Future Directions

6.2.1 Effective Feature Extractor(s)

Feature quality directly affects TSGV performance. Illustrated in the common pipeline (Fig. 3), existing solutions extract visual and textual features independently using corresponding pre-trained visual and textual extractors. Thus there is a large gap between extracted visual and textual features for in different feature spaces. Although TSGV methods attempt to project them into the same feature space, the natural gap between them is hard to be eliminated. There may be also differences between TSGV datasets and the datasets used to pre-train feature extractors, which leads to information loss or inaccurate representations.

Recently, Zhang *et al.* [52] develop a single-stream feature extraction framework for TSGV task, following BERT [37]. Visual and textual features are concatenated and jointly encoded with stacked transformer blocks. However, the visual and textual features remain separately generated by different pre-trained extractors. Xu *et al.* [140] propose a pre-training strategy for TSGV by constructing a large-scale synthesized dataset with TSGV

annotations. Inspired by ViT [167], Cao *et al.* [141] develop a video cubic embedding module to extract 3D visual tokens and learn video content from scratch without reliance on pre-trained visual feature extractor. Although they adopt GloVe [36] embeddings for query, the issues of feature gap are well alleviated. Considering recent advances in video-based vision-language pre-training (*e.g.*, BVET [168], ActBERT [169], ClipBERT [170], and VideoCLIP [171]), dedicated or more effective feature extractors for TSGV are much expected.

6.2.2 TSGV with Multiple Answers

Existing TSGV benchmark datasets generally hold an implicit assumption that there is only one ground-truth moment exist in input video for a query. In reality, a query may describe multiple disjoint moments in a video. Lei *et al.* [166] present a unified benchmark dataset named QVHighlights for both TSGV and highlight detection tasks. Given a query, QVHighlights provides one or multiple disjoint moments in a video, enabling a more realistic evaluation of TSGV methods. The authors then propose Moment-DETR to solve the TSGV as a direct set prediction problem, inspired by DETR [142]. From query perspective, Bao *et al.* [138] convert TSGV to a dense events grounding task, which aims to jointly localize multiple moments described in a paragraph, *i.e.*, multiple queries. Jointly localizing multiple moments could help to alleviate the bias issue in TSGV. This joint localization may also help to improve accuracy as moments are semantically correlated and temporally coordinated by their order in a video. In general, multiple answers for a query is a novel task inherited from the standard TSGV task. The setting is more realistic and less-biased.

6.2.3 Spatio-Temporal Sentence Grounding in Videos

Spatio-temporal sentence grounding in videos (STSGV) is another extension of TSGV. STSGV aims to sequentially localize the referring instances from a sequence of continuous frames in a video, *i.e.*, a spatio-temporal tube, that semantically correspond to the given sentence query. STSGV is more complicated, since the task requires to not only localize the temporal boundaries of the event in video, but also detect bounding boxes among frames within the temporal boundaries. Recently, a series of work [172]–[183] is proposed for this problem. A number of datasets are available, including VID-sentence [174] which is based on ImageNet video object detection, ActivityNet-SRL [176] from existing caption and grounding datasets, VidSTG [177], and HC-STVG [181].

Despite multiple datasets being made available, annotating spatio-temporal tubes from video is even difficult and labor-intensive, compared with TSGV annotation. Thus, many methods [172]–[175], [182] seek to solve STSGV under weakly-supervised setting, which do not require fully annotated dataset. Although some promising results are achieved, STSGV remains under explored and is far apart to be addressed.

6.2.4 Multi-modal Temporal Grounding in Video

TSGV is a form of temporal video grounding using text sentence as query, *i.e.*, language modality. Other modalities, such as audio, image, and short video clip, may also serve as queries for temporal video grounding. In fact, audio-visual event localization (AVEL) [184]–[190] is to retrieve the synchronized video segment for a given audio content from an untrimmed video. The task of Image-to-Video Retrieval (IVR) [191]–[194] localizes video segments that contain similar activity as in a query image. Similarly,

given a query video and a reference video, video re-localization (VRL) [195]–[198] localizes a segment in the reference video that semantically corresponds to the query video. Conceptually, the query is in the form of audio in AVEL, appearance vision in IVR, and motion vision in VRL, respectively. Compared to TSGV, temporal video grounding with such modalities are not fully exploited.

Different query modalities could provide extra guidance to boost performance for moment localization in videos. For instance, audio signals (*e.g.*, dog bark, noise in kitchen) offer auxiliary clues [105], [199] for precise localization. Converting voice in video (if exists) into subtitle texts using ASR [200], [201] could provide relevant information for the cross-modal alignment between video and query. From the perspective of query, different modalities of query (*e.g.*, audio, sentence, and image) that describe the same event could perform cross-validation of the retrieved results. Although TSGV, AVEL, IVR, and VRL accept different input modalities as query, there is lack of a unified framework, which is suitable for all settings.

6.2.5 Video Corpus Moment Retrieval

Video corpus moment retrieval (VCMR) extends video sources for TSGV. Instead of localizing moments in a single video, VCMR aims to retrieve a matching moment to a query from a collection of untrimmed and unsegmented videos. Escorcia *et al.* [202] first extend TSGV to VCMR, and devise clip-query alignment model to compare query features with uniformly partitioned video segments. Lei *et al.* [203] construct the TVR dataset, where videos come with associated textual subtitles. Then Lei *et al.* [204] further extend TVR to a multilingual version named mTVR, containing both English and Chinese queries.

A few recent methods [205]–[210] tackle the VCMR problems. Zhang *et al.* [206] develop a hierarchical multi-modal encoder to learn multimodal interactions at both coarse- and fine-grained granularities. Zhang *et al.* [207] introduce contrastive learning to replace the time-consuming multimodal interaction strategy in VCMR to achieve a balance between efficiency and retrieval accuracy. Hou *et al.* [210] develop a two-step multimodal fusion for precise and efficient moment retrieval.

In general, VCMR contains two sub-tasks, *i.e.*, video retrieval and moment localization. If a TSGV model is directly adapted, the query needs to interact with every video in the corpus, which is infeasible. However, VCMR is more closer to the practical scenarios as videos are ubiquitous.

7 CONCLUSION

Many techniques are available to learn dense representations of various types of data *e.g.*, text, video, and audio. Through multi-modal interaction, cross-modal applications like TSGV become feasible. In this survey, we start with how to extract features from text and video, then focus on the interaction between the two types of features for TSGV. Although TSGV has a short history, we have seen the trend of development from sliding window methods, to proposal-based and proposal-free methods, then different views of the task with solutions from reinforcement learning and weakly-supervised learning. At the same time, we also see the challenges in this field; hence results obtained on benchmark datasets may not necessarily reflect a model’s performance in reality. Addressing these challenges would certainly brings in improvements to current solutions. Further, as a fundamental task, solutions to

TSGV directly benefit many more related applications like spatio-temporal sentence grounding in videos, and video corpus moment retrieval. We hope this survey could serve as a good reference for researchers working on these interesting problems.

REFERENCES

- [1] D. Tran, L. Bourdev, R. Fergus, L. Torresani, and M. Paluri, "Learning spatiotemporal features with 3d convolutional networks," in *ICCV*, 2015.
- [2] C. Feichtenhofer, A. Pinz, and A. Zisserman, "Convolutional two-stream network fusion for video action recognition," in *CVPR*, 2016.
- [3] J. Carreira and A. Zisserman, "Quo vadis, action recognition? a new model and the kinetics dataset," in *CVPR*, 2017.
- [4] M. Xu, C. Zhao, D. S. Rojas, A. Thabet, and B. Ghanem, "G-tad: Sub-graph localization for temporal action detection," in *CVPR*, 2020.
- [5] W. Wang, N. Yang, F. Wei, B. Chang, and M. Zhou, "Gated self-matching networks for reading comprehension and question answering," in *ACL*, 2017.
- [6] M. Seo, A. Kembhavi, A. Farhadi, and H. Hajishirzi, "Bidirectional attention flow for machine comprehension," in *ICLR*, 2017.
- [7] A. W. Yu, D. Dohan, Q. Le, T. Luong, R. Zhao, and K. Chen, "Fast and accurate reading comprehension by combining self-attention and convolution," in *ICLR*, 2018.
- [8] H. Huang, C. Zhu, Y. Shen, and W. Chen, "Fusionnet: Fusing via fully-aware attention with application to machine comprehension," in *ICLR*, 2018.
- [9] J. Gao, C. Sun, Z. Yang, and R. Nevatia, "Tall: Temporal activity localization via language query," in *ICCV*, 2017.
- [10] L. A. Hendricks, O. Wang, E. Shechtman, J. Sivic, T. Darrell, and B. Russell, "Localizing moments in video with natural language," in *ICCV*, 2017.
- [11] M. Liu, X. Wang, L. Nie, Q. Tian, B. Chen, and T.-S. Chua, "Cross-modal moment localization in videos," in *ACM MM*, 2018.
- [12] M. Liu, X. Wang, L. Nie, X. He, B. Chen, and T.-S. Chua, "Attentive moment retrieval in videos," in *SIGIR*, 2018.
- [13] R. Ge, J. Gao, K. Chen, and R. Nevatia, "Mac: Mining activity concepts for language-based temporal localization," in *WACV*, 2019.
- [14] H. Xu, K. He, L. Sigal, S. Sclaroff, and K. Saenko, "Text-to-clip video retrieval with early fusion and re-captioning," *ArXiv*, vol. abs/1804.05113, 2018.
- [15] J. Chen, X. Chen, L. Ma, Z. Jie, and T.-S. Chua, "Temporally grounding natural sentence in video," in *EMNLP*, 2018.
- [16] D. Zhang, X. Dai, X. Wang, Y.-F. Wang, and L. S. Davis, "Man: Moment alignment network for natural language moment retrieval via iterative graph adjustment," in *CVPR*, 2019.
- [17] Y. Yuan, L. Ma, J. Wang, W. Liu, and W. Zhu, "Semantic conditioned dynamic modulation for temporal sentence grounding in videos," in *NeurIPS*, 2019.
- [18] S. Zhang, H. Peng, J. Fu, and J. Luo, "Learning 2d temporal adjacent networks formoment localization with natural language," in *AAAI*, vol. 34, 2020.
- [19] Y. Yuan, T. Mei, and W. Zhu, "To find where you talk: Temporal sentence localization in video with attention based location regression," in *AAAI*, vol. 33, 2019.
- [20] S. Ghosh, A. Agarwal, Z. Parekh, and A. Hauptmann, "ExCL: Extractive Clip Localization Using Natural Language Descriptions," in *NAACL*, 2019.
- [21] J. Chen, L. Ma, X. Chen, Z. Jie, and J. Luo, "Localizing natural language in videos," in *AAAI*, vol. 33, 2019.
- [22] C. Lu, L. Chen, C. Tan, X. Li, and J. Xiao, "DEBUG: A dense bottom-up grounding approach for natural language video localization," in *EMNLP*, 2019.
- [23] H. Zhang, A. Sun, W. Jing, and J. T. Zhou, "Span-based localizing network for natural language video localization," in *ACL*, 2020.
- [24] D. He, X. Zhao, J. Huang, F. Li, X. Liu, and S. Wen, "Read, watch, and move: Reinforcement learning for temporally grounding natural language descriptions in videos," in *AAAI*, vol. 33, 2019.
- [25] W. Wang, Y. Huang, and L. Wang, "Language-driven temporal activity localization: A semantic matching reinforcement learning model," in *CVPR*, 2019.
- [26] J. Wu, G. Li, S. Liu, and L. Lin, "Tree-structured policy based progressive reinforcement learning for temporally language grounding in video," in *AAAI*, vol. 34, 2020.
- [27] N. C. Mithun, S. Paul, and A. K. Roy-Chowdhury, "Weakly supervised video moment retrieval from text queries," in *CVPR*, 2019.
- [28] M. Gao, L. Davis, R. Socher, and C. Xiong, "WSLLN: weakly supervised natural language localization networks," in *EMNLP*, 2019.
- [29] X. Duan, W. Huang, C. Gan, J. Wang, W. Zhu, and J. Huang, "Weakly supervised dense event captioning in videos," in *NeurIPS*, vol. 31, 2018.
- [30] Z. Lin, Z. Zhao, Z. Zhang, Q. Wang, and H. Liu, "Weakly-supervised video moment retrieval via semantic completion network," in *AAAI*, vol. 34, 2020.
- [31] S. Chen and Y.-G. Jiang, "Towards bridging event captioner and sentence localizer for weakly supervised dense event captioning," in *CVPR*, 2021.
- [32] Y. Yang, Z. Li, and G. Zeng, "A survey of temporal activity localization via language in untrimmed videos," in *ICCV*, 2020.
- [33] X. Liu, X. Nie, Z. Tan, J. Guo, and Y. Yin, "A survey on natural language video localization," *ArXiv*, vol. abs/2104.00234, 2021.
- [34] X. Lan, Y. Yuan, X. Wang, Z. Wang, and W. Zhu, "A survey on temporal sentence grounding in videos," *ArXiv*, vol. abs/2109.08039, 2021.
- [35] T. Mikolov, K. Chen, G. Corrado, and J. Dean, "Efficient estimation of word representations in vector space," *ArXiv*, vol. abs/1301.3781, 2013.
- [36] J. Pennington, R. Socher, and C. Manning, "GloVe: Global vectors for word representation," in *EMNLP*, 2014.
- [37] J. Devlin, M.-W. Chang, K. Lee, and K. Toutanova, "BERT: Pre-training of deep bidirectional transformers for language understanding," in *NAACL*, 2019.
- [38] Y. Liu, M. Ott, N. Goyal, J. Du, M. Joshi, D. Chen, O. Levy, M. Lewis, L. Zettlemoyer, and V. Stoyanov, "Roberta: A robustly optimized bert pretraining approach," *ArXiv*, vol. abs/1907.11692, 2019.
- [39] R. Kiros, Y. Zhu, R. R. Salakhutdinov, R. Zemel, R. Urtasun, A. Torralba, and S. Fidler, "Skip-thought vectors," in *NeurIPS*, vol. 28, 2015.
- [40] A. Conneau, D. Kiela, H. Schwenk, L. Barrault, and A. Bordes, "Supervised learning of universal sentence representations from natural language inference data," in *EMNLP*, 2017.
- [41] N. Reimers and I. Gurevych, "Sentence-BERT: Sentence embeddings using Siamese BERT-networks," in *EMNLP*, 2019.
- [42] K. Simonyan and A. Zisserman, "Very deep convolutional networks for large-scale image recognition," *ArXiv*, vol. abs/1409.1556, 2014.
- [43] K. He, X. Zhang, S. Ren, and J. Sun, "Deep residual learning for image recognition," in *CVPR*, 2016.
- [44] A. Wu and Y. Han, "Multi-modal circulant fusion for video-to-language and backward," in *IJCAI*, 2018.
- [45] H. Xu, K. He, B. A. Plummer, L. Sigal, S. Sclaroff, and K. Saenko, "Multilevel language and vision integration for text-to-clip retrieval," in *AAAI*, vol. 33, 2019.
- [46] S. Chen and Y.-G. Jiang, "Semantic proposal for activity localization in videos via sentence query," in *AAAI*, vol. 33, 2019.
- [47] S. Xiao, L. Chen, S. Zhang, W. Ji, J. Shao, L. Ye, and J. Xiao, "Boundary proposal network for two-stage natural language video localization," in *AAAI*, vol. 35, 2021.
- [48] D. Liu, X. Qu, J. Dong, and P. Zhou, "Adaptive proposal generation network for temporal sentence localization in videos," in *EMNLP*, 2021.
- [49] H. Xu, A. Das, and K. Saenko, "R-c3d: Region convolutional 3d network for temporal activity detection," in *ICCV*, 2017.
- [50] Z. Zhang, Z. Lin, Z. Zhao, and Z. Xiao, "Cross-modal interaction networks for query-based moment retrieval in videos," in *SIGIR*, 2019.
- [51] Y. Yuan, L. Ma, J. Wang, W. Liu, and W. Zhu, "Semantic conditioned dynamic modulation for temporal sentence grounding in videos," *IEEE TPAMI*, vol. 1, 2020.
- [52] M. Zhang, Y. Yang, X. Chen, Y. Ji, X. Xu, J. Li, and H. T. Shen, "Multi-stage aggregated transformer network for temporal language localization in videos," in *CVPR*, 2021.
- [53] H. Wang, Z.-J. Zha, L. Li, D. Liu, and J. Luo, "Structured multi-level interaction network for video moment localization via language query," in *CVPR*, 2021.
- [54] J. Gao, X. Sun, M. Xu, X. Zhou, and B. Ghanem, "Relation-aware video reading comprehension for temporal language grounding," in *EMNLP*, 2021.
- [55] J. Gao and C. Xu, "Fast video moment retrieval," in *ICCV*, 2021.
- [56] B. Thomee, D. A. Shamma, G. Friedland, B. Elizalde, K. Ni, D. Poland, D. Borth, and L.-J. Li, "Yfcc100m: The new data in multimedia research," *Communications of the ACM*, vol. 59, 2016.
- [57] L. A. Hendricks, O. Wang, E. Shechtman, J. Sivic, T. Darrell, and B. Russell, "Localizing moments in video with temporal language," in *EMNLP*, 2018.
- [58] G. A. Sigurdsson, G. Varol, X. Wang, A. Farhadi, I. Laptev, and A. Gupta, "Hollywood in homes: Crowdsourcing data collection for activity understanding," in *ECCV*, 2016.

- [59] C. Manning, M. Surdeanu, J. Bauer, J. Finkel, S. Bethard, and D. McClosky, "The Stanford CoreNLP natural language processing toolkit," in *ACL: System Demonstrations*, 2014.
- [60] R. Krishna, K. Hata, F. Ren, L. Fei-Fei, and J. C. Niebles, "Dense-captioning events in videos," in *ICCV*, 2017.
- [61] F. C. Heilbron, V. Escorcia, B. Ghanem, and J. C. Niebles, "Activitynet: A large-scale video benchmark for human activity understanding," in *CVPR*, 2015.
- [62] M. Regneri, M. Rohrbach, D. Wetzels, S. Thater, B. Schiele, and M. Pinkal, "Grounding action descriptions in videos," *TACL*, vol. 1, 2013.
- [63] M. Rohrbach, M. Regneri, M. Andriluka, S. Amin, M. Pinkal, and B. Schiele, "Script data for attribute-based recognition of composite activities," in *ECCV*, 2012.
- [64] M. Soldan, A. Pardo, J. L. Alcázar, F. C. Heilbron, C. Zhao, S. Giancola, and B. Ghanem, "Mad: A scalable dataset for language grounding in videos from movie audio descriptions," *ArXiv*, vol. abs/2112.00431, 2021.
- [65] H. Zhang, A. Sun, W. Jing, L. Zhen, J. T. Zhou, and R. S. M. Goh, "Natural language video localization: A revisit in span-based question answering framework," *IEEE TPAMI*, vol. 1, 2021.
- [66] R. Girshick, J. Donahue, T. Darrell, and J. Malik, "Rich feature hierarchies for accurate object detection and semantic segmentation," in *CVPR*, 2014.
- [67] S. Ren, K. He, R. Girshick, and J. Sun, "Faster r-cnn: Towards real-time object detection with region proposal networks," *IEEE TPAMI*, vol. 39, 2017.
- [68] T.-Y. Lin, P. Goyal, R. Girshick, K. He, and P. Dollár, "Focal loss for dense object detection," *IEEE TPAMI*, vol. 42, 2020.
- [69] R. Hu, H. Xu, M. Rohrbach, J. Feng, K. Saenko, and T. Darrell, "Natural language object retrieval," in *CVPR*, 2016.
- [70] Y. Yuan, X. Lan, X. Wang, L. Chen, Z. Wang, and W. Zhu, "A closer look at temporal sentence grounding in videos: Dataset and metric," in *ACM HUMA*, 2021.
- [71] S. Zhang, J. Su, and J. Luo, "Exploiting temporal relationships in video moment localization with natural language," in *ACM MM*, 2019.
- [72] K. Ning, M. Cai, D. Xie, and F. Wu, "An attentive sequence to sequence translator for localizing video clips by natural language," *IEEE TMM*, vol. 22, 2020.
- [73] B. Jiang, X. Huang, C. Yang, and J. Yuan, "Cross-modal video moment retrieval with spatial and language-temporal attention," in *ACM ICMR*, 2019.
- [74] Y. Zeng, D. Cao, X. Wei, M. Liu, Z. Zhao, and Z. Qin, "Multi-modal relational graph for cross-modal video moment retrieval," in *CVPR*, 2021.
- [75] K. Ning, L. Xie, J. Liu, F. Wu, and Q. Tian, "Interaction-integrated network for natural language moment localization," *IEEE TIP*, vol. 30, 2021.
- [76] S. Xiao, L. Chen, J. Shao, Y. Zhuang, and J. Xiao, "Natural language video localization with learnable moment proposals," in *EMNLP*, 2021.
- [77] Y. Hu, M. Liu, X. Su, Z. Gao, and L. Nie, "Video moment localization via deep cross-modal hashing," *IEEE TIP*, vol. 30, 2021.
- [78] Z. Lin, Z. Zhao, Z. Zhang, Z. Zhang, and D. Cai, "Moment retrieval via cross-modal interaction networks with query reconstruction," *IEEE TIP*, vol. 29, 2020.
- [79] J. Wang, L. Ma, and W. Jiang, "Temporally grounding language queries in videos by contextual boundary-aware prediction," in *AAAI*, 2020.
- [80] X. Qu, P. Tang, Z. Zou, Y. Cheng, J. Dong, P. Zhou, and Z. Xu, "Fine-grained iterative attention network for temporal language localization in videos," in *ACM MM*, 2020.
- [81] Z. Ma, X. Han, X. Song, Y. Cui, and L. Nie, "Hierarchical deep residual reasoning for temporal moment localization," in *ACM MM Asia*, 2021.
- [82] Z. Zhang, X. Han, X. Song, Y. Yan, and L. Nie, "Multi-modal interaction graph convolutional network for temporal language localization in videos," *IEEE TIP*, vol. 30, 2021.
- [83] D. Liu, X. Qu, X.-Y. Liu, J. Dong, P. Zhou, and Z. Xu, "Jointly cross- and self-modal graph attention network for query-based moment localization," in *ACM MM*, 2020.
- [84] D. Liu, X. Qu, J. Dong, and P. Zhou, "Reasoning step-by-step: Temporal sentence localization in videos via deep rectification-modulation network," in *COLING*, 2020.
- [85] D. Liu, X. Qu, and P. Zhou, "Progressively guide to attend: An iterative alignment framework for temporal sentence grounding," in *EMNLP*, 2021.
- [86] W. Wang, J. Cheng, and S. Liu, "Dct-net: A deep co-interactive transformer network for video temporal grounding," *Image and Vision Computing*, vol. 110, 2021.
- [87] B. Liu, S. Yeung, E. Chou, D.-A. Huang, L. Fei-Fei, and J. C. Niebles, "Temporal modular networks for retrieving complex compositional activities in videos," in *ECCV*, 2018.
- [88] S. Zhang, H. Peng, J. Fu, Y. Lu, and J. Luo, "Multi-scale 2d temporal adjacency networks for moment localization with natural language," *IEEE TPAMI*, 2021.
- [89] Q. Zheng, J. Dong, X. Qu, X. Yang, S. Ji, and X. Wang, "Progressive localization networks for language-based moment localization," *ArXiv*, vol. abs/2102.01282, 2021.
- [90] Y. Hu, L. Nie, M. Liu, K. Wang, Y. Wang, and X.-S. Hua, "Coarse-to-fine semantic alignment for cross-modal moment localization," *IEEE TIP*, vol. 30, 2021.
- [91] Z. Jia, M. Dong, J. Ru, L. Xue, S. Yang, and C. Li, "Stcm-net: A symmetrical one-stage network for temporal language localization in videos," *Neurocomputing*, vol. 471, 2022.
- [92] M. Soldan, M. Xu, S. Qu, J. Tegner, and B. Ghanem, "Vlg-net: Video-language graph matching network for video grounding," in *ICCV*, 2021.
- [93] Q. Huang, J. Wei, Y. Cai, C. Zheng, J. Chen, H.-f. Leung, and Q. Li, "Aligned dual channel graph convolutional network for visual question answering," in *ACL*, 2020.
- [94] Z. Wu, J. Gao, S. Huang, and C. Xu, "Diving into the relations: Leveraging semantic and visual structures for video moment retrieval," in *ICME*, 2021.
- [95] P. Shi and J. Lin, "Simple bert models for relation extraction and semantic role labeling," *ArXiv*, vol. abs/1904.05255, 2019.
- [96] Z. Wang, L. Wang, T. Wu, T. Li, and G. Wu, "Negative sample matters: A renaissance of metric learning for temporal grounding," *ArXiv*, vol. abs/2109.04872, 2021.
- [97] L. Chen, C. Lu, S. Tang, J. Xiao, D. Zhang, C. Tan, and X. Li, "Re-thinking the bottom-up framework for query-based video localization," in *AAAI*, vol. 34, 2020.
- [98] B. Zhang, Y. Li, C. Yuan, D. Xu, P. Jiang, and Y. Shan, "A simple yet effective method for video temporal grounding with cross-modality attention," *ArXiv*, vol. abs/2009.11232, 2020.
- [99] R. Zeng, H. Xu, W. Huang, P. Chen, M. Tan, and C. Gan, "Dense regression network for video grounding," in *CVPR*, 2020.
- [100] J. Mun, M. Cho, and B. Han, "Local-global video-text interactions for temporal grounding," in *CVPR*, 2020.
- [101] K. Li, D. Guo, and M. Wang, "Proposal-free video grounding with contextual pyramid network," in *AAAI*, vol. 35, 2021.
- [102] H. Zhou, C. Zhang, Y. Luo, Y. Chen, and C. Hu, "Embracing uncertainty: Decoupling and de-bias for robust temporal grounding," in *CVPR*, 2021.
- [103] X. Liu, X. Nie, J. Teng, L. Lian, and Y. Yin, "Single-shot semantic matching network for moment localization in videos," *ACM TOMCCAP*, vol. 17, 2021.
- [104] S. Chen and Y.-G. Jiang, "Hierarchical visual-textual graph for temporal activity localization via language," in *ECCV*, 2020.
- [105] S. Chen, W. Jiang, W. Liu, and Y.-G. Jiang, "Learning modality interaction for temporal sentence localization and event captioning in videos," in *ECCV*, 2020.
- [106] Y.-W. Chen, Y.-H. Tsai, and M.-H. Yang, "End-to-end multi-modal video temporal grounding," in *NeurIPS*, vol. 34, 2021.
- [107] Y. Aytar, C. Vondrick, and A. Torralba, "Soundnet: Learning sound representations from unlabeled video," in *NeurIPS*, vol. 29, 2016.
- [108] C. Clark and M. Gardner, "Simple and effective multi-paragraph reading comprehension," in *ACL*, 2018.
- [109] C. Rodriguez, E. Marrese-Taylor, F. S. Saleh, H. LI, and S. Gould, "Proposal-free temporal moment localization of a natural-language query in video using guided attention," in *WACV*, 2020.
- [110] H. Zhang, A. Sun, W. Jing, L. Zhen, J. T. Zhou, and S. M. R. Goh, "Parallel attention network with sequence matching for video grounding," in *Findings of ACL*, 2021.
- [111] Y. Zhao, Z. Zhao, Z. Zhang, and Z. Lin, "Cascaded prediction network via segment tree for temporal video grounding," in *CVPR*, 2021.
- [112] G. Nan, R. Qiao, Y. Xiao, J. Liu, S. Leng, H. Zhang, and W. Lu, "Interventional video grounding with dual contrastive learning," in *CVPR*, 2021.
- [113] G. Liang, S. Ji, and Y. Zhang, "Local-enhanced interaction for temporal moment localization," in *ACM ICMR*, 2021.
- [114] X. Yu, M. Malmir, X. He, J. Chen, T. Wang, Y. Wu, Y. Liu, and Y. Liu, "Cross interaction network for natural language guided video moment retrieval," in *SIGIR*, 2021.
- [115] H. Tang, J. Zhu, L. Wang, Q. Zheng, and T. Zhang, "Multi-level query interaction for temporal language grounding," *IEEE TITS*, 2021.
- [116] H. Tang, J. Zhu, M. Liu, Z. Gao, and Z. Cheng, "Frame-wise cross-modal matching for video moment retrieval," *IEEE TMM*, 2021.

- [117] Z. Zhang, Z. Zhao, Z. Zhang, Z. Lin, Q. Wang, and R. Hong, "Temporal textual localization in video via adversarial bi-directional interaction networks," *IEEE TMM*, vol. 23, 2021.
- [118] S. Qi, L. Yang, C. Li, and Y. Huang, "Collaborative spatial-temporal interaction for language-based moment retrieval," in *WCSP*, 2021.
- [119] C. Rodriguez-Opazo, E. Marrese-Taylor, B. Fernando, H. Li, and S. Gould, "Dori: Discovering object relationships for moment localization of a natural language query in a video," in *WACV*, 2021.
- [120] D. Liu, X. Qu, J. Dong, P. Zhou, Y. Cheng, W. Wei, Z. Xu, and Y. Xie, "Context-aware biaffine localizing network for temporal sentence grounding," in *CVPR*, 2021.
- [121] L. Zhang and R. J. Radke, "Natural language video moment localization through query-controlled temporal convolution," in *WACV*, 2022.
- [122] X. Ma and E. Hovy, "End-to-end sequence labeling via bi-directional lstm-cnns-crf," in *ACL*, 2016.
- [123] J. T. Zhou, H. Zhang, D. Jin, H. Zhu, M. Fang, R. S. M. Goh, and K. Kwok, "Dual adversarial neural transfer for low-resource named entity recognition," in *ACL*, 2019.
- [124] J. Yu, B. Bohnet, and M. Poesio, "Named entity recognition as dependency parsing," in *ACL*, 2020.
- [125] J. Pearl, M. Glymour, and N. P. Jewell, *Causal inference in statistics: A primer*. John Wiley & Sons, 2016.
- [126] R. S. Sutton and A. G. Barto, *Reinforcement learning: An introduction*. MIT press, 2018.
- [127] A. Shapiro, "Monte carlo sampling methods," *Handbooks in operations research and management science*, vol. 10, 2003.
- [128] D. Li, H. Wu, J. Zhang, and K. Huang, "A2-rl: Aesthetics aware reinforcement learning for image cropping," in *CVPR*, 2018.
- [129] D. Cao, Y. Zeng, X. Wei, L. Nie, R. Hong, and Z. Qin, "Adversarial video moment retrieval by jointly modeling ranking and localization," in *ACM MM*, 2020.
- [130] D. Cao, Y. Zeng, M. Liu, X. He, M. Wang, and Z. Qin, "Strong: Spatio-temporal reinforcement learning for cross-modal video moment localization," in *ACM MM*, 2020.
- [131] M. Hahn, A. Kadav, J. M. Rehg, and H. P. Graf, "Tripping through time: Efficient localization of activities in videos," in *BMVC*, 2020.
- [132] X. Sun, H. Wang, and B. He, "Maban: Multi-agent boundary-aware network for natural language moment retrieval," *IEEE TIP*, vol. 30, 2021.
- [133] D. Shao, Y. Xiong, Y. Zhao, Q. Huang, Y. Qiao, and D. Lin, "Find and focus: Retrieve and localize video events with natural language queries," in *ECCV*, 2018.
- [134] Y. Zhao, Y. Xiong, L. Wang, Z. Wu, X. Tang, and D. Lin, "Temporal action detection with structured segment networks," in *ICCV*, 2017.
- [135] H. Wang, Z.-J. Zha, X. Chen, Z. Xiong, and J. Luo, "Dual path interaction network for video moment localization," in *ACM MM*, 2020.
- [136] M. Patrick, P.-Y. Huang, Y. Asano, F. Metzger, A. G. Hauptmann, J. F. Henriques, and A. Vedaldi, "Support-set bottlenecks for video-text representation learning," in *ICLR*, 2021.
- [137] X. Ding, N. Wang, S. Zhang, D. Cheng, X. Li, Z. Huang, M. Tang, and X. Gao, "Support-set based cross-supervision for video grounding," in *ICCV*, 2021.
- [138] P. Bao, Q. Zheng, and Y. Mu, "Dense events grounding in video," in *AAAI*, vol. 35, 2021.
- [139] W. Gou, W. Shi, J. Lou, L. Huang, P. Zhou, and R. Li, "Sneak: Synonymous sentences-aware adversarial attack on natural language video localization," *ArXiv*, vol. abs/2112.04154, 2021.
- [140] M. Xu, J.-M. Pérez-Rúa, V. Escorcía, B. Martínez, X. Zhu, L. Zhang, B. Ghanem, and T. Xiang, "Boundary-sensitive pre-training for temporal localization in videos," in *ICCV*, 2021.
- [141] M. Cao, L. Chen, M. Z. Shou, C. Zhang, and Y. Zou, "On pursuit of designing multi-modal transformer for video grounding," in *EMNLP*, 2021.
- [142] N. Carion, F. Massa, G. Synnaeve, N. Usunier, A. Kirillov, and S. Zagoruyko, "End-to-end object detection with transformers," in *ECCV*, 2020.
- [143] Z. Chen, L. Ma, W. Luo, P. Tang, and K.-Y. K. Wong, "Look closer to ground better: Weakly-supervised temporal grounding of sentence in video," *ArXiv*, vol. abs/2001.09308, 2020.
- [144] M. Ma, S. Yoon, J. Kim, Y. Lee, S. Kang, and C. D. Yoo, "Vlanet: Video-language alignment network for weakly-supervised video moment retrieval," in *ECCV*, 2020.
- [145] J. Wu, G. Li, X. Han, and L. Lin, "Reinforcement learning for weakly supervised temporal grounding of natural language in untrimmed videos," in *ACM MM*, 2020.
- [146] Z. Zhang, Z. Zhao, Z. Lin, J. Zhu, and X. He, "Counterfactual contrastive learning for weakly-supervised vision-language grounding," in *NeurIPS*, vol. 33, 2020.
- [147] C. Da, Y. Zhang, Y. Zheng, P. Pan, Y. Xu, and C. Pan, "Asynce: Disentangling false-positives for weakly-supervised video grounding," in *ACM MM*, 2021.
- [148] Z. Wang, J. Chen, and Y.-G. Jiang, "Visual co-occurrence alignment learning for weakly-supervised video moment retrieval," in *ACM MM*, 2021.
- [149] Y. Wang, W. Zhou, and H. Li, "Fine-grained semantic alignment network for weakly supervised temporal language grounding," in *Findings of EMNLP*, 2021.
- [150] J. Huang, Y. Liu, S. Gong, and H. Jin, "Cross-sentence temporal and semantic relations in video activity localisation," in *ICCV*, 2021.
- [151] W. Yang, T. Zhang, Y. Zhang, and F. Wu, "Local correspondence network for weakly supervised temporal sentence grounding," *IEEE TIP*, vol. 30, 2021.
- [152] J. Teng, X. Lu, Y. Gong, X. Liu, X. Nie, and Y. Yin, "Regularized two granularity loss function for weakly supervised video moment retrieval," *IEEE TMM*, 2021.
- [153] Y. Wang, J. Deng, W. Zhou, and H. Li, "Weakly supervised temporal adjacent network for language grounding," *IEEE TMM*, 2021.
- [154] R. Tan, H. Xu, K. Saenko, and B. A. Plummer, "Logan: Latent graph co-attention network for weakly-supervised video moment retrieval," in *WACV*, 2021.
- [155] Y. Song, J. Wang, L. Ma, Z. Yu, and J. Yu, "Weakly-supervised multi-level attentional reconstruction network for grounding textual queries in videos," *ArXiv*, vol. abs/2003.07048, 2020.
- [156] T. Lin, X. Liu, X. Li, E. Ding, and S. Wen, "Bmn: Boundary-matching network for temporal action proposal generation," in *ICCV*, 2019.
- [157] S. Chen, "Towards bridging video and language by caption generation and sentence localization," in *ACM MM*, 2021.
- [158] Z. Zhang, Z. Lin, Z. Zhao, J. Zhu, and X. He, "Regularized two-branch proposal networks for weakly-supervised moment retrieval in videos," in *ACM MM*, 2020.
- [159] F. Luo, S. Chen, J. Chen, Z. Wu, and Y.-G. Jiang, "Self-supervised learning for semi-supervised temporal language grounding," *ArXiv*, vol. abs/2109.11475, 2021.
- [160] J. Nam, D. Ahn, D. Kang, S. J. Ha, and J. Choi, "Zero-shot natural language video localization," in *ICCV*, 2021.
- [161] J. Gao and C. Xu, "Learning video moment retrieval without a single annotated video," *IEEE TCSVT*, 2021.
- [162] C. Szegedy, S. Ioffe, V. Vanhoucke, and A. A. Alemi, "Inception-v4, inception-resnet and the impact of residual connections on learning," in *AAAI*, 2017.
- [163] M. Otani, Y. Nakahima, E. Rahtu, and J. Heikkilä, "Uncovering hidden challenges in query-based video moment retrieval," in *BMVC*, 2020.
- [164] X. Yang, F. Feng, W. Ji, M. Wang, and T.-S. Chua, "Deconfounded video moment retrieval with causal intervention," in *SIGIR*, 2021.
- [165] H. Zhang, A. Sun, W. Jing, and J. T. Zhou, "Towards debiasing temporal sentence grounding in video," *ArXiv preprint arXiv:2111.04321*, vol. abs/2111.04321, 2021.
- [166] J. Lei, T. L. Berg, and M. Bansal, "Qvhighlights: Detecting moments and highlights in videos via natural language queries," in *NeurIPS*, 2021.
- [167] A. Dosovitskiy, L. Beyer, A. Kolesnikov, D. Weissenborn, X. Zhai, T. Unterthiner, M. Dehghani, M. Minderer, G. Heigold, S. Gelly, J. Uszkoreit, and N. Houlsby, "An image is worth 16x16 words: Transformers for image recognition at scale," in *ICLR*, 2021.
- [168] R. Wang, D. Chen, Z. Wu, Y. Chen, X. Dai, M. Liu, Y.-G. Jiang, L. Zhou, and L. Yuan, "Bevt: Bert pretraining of video transformers," *ArXiv*, vol. abs/2112.01529, 2021.
- [169] L. Zhu and Y. Yang, "Actbert: Learning global-local video-text representations," in *CVPR*, 2020.
- [170] J. Lei, L. Li, L. Zhou, Z. Gan, T. L. Berg, M. Bansal, and J. Liu, "Less is more: Clipbert for video-and-language learning via sparse sampling," in *CVPR*, 2021.
- [171] H. Xu, G. Ghosh, P.-Y. Huang, D. Okhonko, A. Aghajanyan, F. Metzger, L. Zettlemoyer, and C. Feichtenhofer, "Videoclip: Contrastive pre-training for zero-shot video-text understanding," *ArXiv*, vol. abs/2109.14084, 2021.
- [172] D.-A. Huang, S. Buch, L. Dery, A. Garg, L. Fei-Fei, and J. C. Niebles, "Finding 'it': Weakly-supervised reference-aware visual grounding in instructional videos," in *CVPR*, 2018.
- [173] J. Shi, J. Xu, B. Gong, and C. Xu, "Not all frames are equal: Weakly-supervised video grounding with contextual similarity and visual clustering losses," in *CVPR*, 2019.

- [174] Z. Chen, L. Ma, W. Luo, and K.-Y. K. Wong, “Weakly-supervised spatio-temporally grounding natural sentence in video,” in *ACL*, 2019.
- [175] J. Chen, W. Bao, and Y. Kong, “Activity-driven weakly-supervised spatio-temporal grounding from untrimmed videos,” in *ACM MM*, 2020.
- [176] A. Sadhu, K. Chen, and R. Nevatia, “Video object grounding using semantic roles in language description,” in *CVPR*, 2020.
- [177] Z. Zhang, Z. Zhao, Y. Zhao, Q. Wang, H. Liu, and L. Gao, “Where does it exist: Spatio-temporal video grounding for multi-form sentences,” in *CVPR*, 2020.
- [178] Z. Zhang, Z. Zhao, Z. Lin, B. Huai, and J. Yuan, “Object-aware multi-branch relation networks for spatio-temporal video grounding,” in *IJCAI*, 2020.
- [179] K. Shen, L. Wu, F. Xu, S. Tang, J. Xiao, and Y. Zhuang, “Hierarchical attention based spatial-temporal graph-to-sequence learning for grounded video description,” in *IJCAI*, 2020.
- [180] Q. Feng, Y. Wei, M. Cheng, and Y. Yang, “Decoupled spatial temporal graphs for generic visual grounding,” *ArXiv*, vol. abs/2103.10191, 2021.
- [181] Z. Tang, Y. Liao, S. Liu, G. Li, X. Jin, H. Jiang, Q. Yu, and D. Xu, “Human-centric spatio-temporal video grounding with visual transformers,” *IEEE TCSVT*, 2021.
- [182] R. Tan, B. Plummer, K. Saenko, H. Jin, and B. Russell, “Look at what i’m doing: Self-supervised spatial grounding of narrations in instructional videos,” in *NeurIPS*, vol. 34, 2021.
- [183] R. Su, Q. Yu, and D. Xu, “Stvgbert: A visual-linguistic transformer based framework for spatio-temporal video grounding,” in *ICCV*, 2021.
- [184] Y. Tian, J. Shi, B. Li, Z. Duan, and C. Xu, “Audio-visual event localization in unconstrained videos,” in *ECCV*, 2018.
- [185] Y. Wu, L. Zhu, Y. Yan, and Y. Yang, “Dual attention matching for audio-visual event localization,” in *ICCV*, 2019.
- [186] H. Xu, R. Zeng, Q. Wu, M. Tan, and C. Gan, “Cross-modal relation-aware networks for audio-visual event localization,” in *ACM MM*, 2020.
- [187] H. Xuan, Z. Zhang, S. Chen, J. Yang, and Y. Yan, “Cross-modal attention network for temporal inconsistent audio-visual event localization,” in *AAAI*, vol. 34, 2020.
- [188] B. Duan, H. Tang, W. Wang, Z. Zong, G. Yang, and Y. Yan, “Audio-visual event localization via recursive fusion by joint co-attention,” in *WACV*, 2021.
- [189] H. Xuan, L. Luo, Z. Zhang, J. Yang, and Y. Yan, “Discriminative cross-modality attention network for temporal inconsistent audio-visual event localization,” *IEEE TIP*, vol. 30, 2021.
- [190] C. Xue, X. Zhong, M. Cai, H. Chen, and W. Wang, “Audio-visual event localization by learning spatial and semantic co-attention,” *IEEE TMM*, 2021.
- [191] N. Garcia and G. Vogiatzis, “Asymmetric spatio-temporal embeddings for large-scale image-to-video retrieval,” in *BMVC*, 2018.
- [192] Z. Zhang, Z. Zhao, Z. Lin, J. Song, and D. Cai, “Localizing unseen activities in video via image query,” in *IJCAI*, 2019.
- [193] R. Xu, L. Niu, J. Zhang, and L. Zhang, “A proposal-based approach for activity image-to-video retrieval,” in *AAAI*, vol. 34, 2020.
- [194] L. Liu, J. Li, L. Niu, R. Xu, and L. Zhang, “Activity image-to-video retrieval by disentangling appearance and motion,” in *AAAI*, vol. 35, 2021.
- [195] Y. Feng, L. Ma, W. Liu, T. Zhang, and J. Luo, “Video re-localization,” in *ECCV*, 2018.
- [196] Y. Feng, L. Ma, W. Liu, and J. Luo, “Spatio-temporal video re-localization by warp lstm,” in *CVPR*, 2019.
- [197] Y.-H. Huang, K.-J. Hsu, S.-K. Jeng, and Y.-Y. Lin, “Weakly-supervised video re-localization with multiscale attention model,” in *AAAI*, vol. 34, 2020.
- [198] C. Jiang, K. Huang, S. He, X. Yang, W. Zhang, X. Zhang, Y. Cheng, L. Yang, Q. Wang, F. Xu, T. Pan, and W. Chu, “Learning segment similarity and alignment in large-scale content based video retrieval,” in *ACM MM*, 2021.
- [199] T. Afouras, J. S. Chung, A. Senior, O. Vinyals, and A. Zisserman, “Deep audio-visual speech recognition,” *IEEE TPAMI*, 2018.
- [200] A. Koenecke, A. Nam, E. Lake, J. Nudell, M. Quartey, Z. Mengesha, C. Troups, J. R. Rickford, D. Jurafsky, and S. Goel, “Racial disparities in automated speech recognition,” *National Academy of Sciences*, vol. 117, 2020.
- [201] H. Huang, F. Xue, H. Wang, and Y. Wang, “Deep graph random process for relational-thinking-based speech recognition,” in *ICML*, vol. 119, 2020.
- [202] V. Escorcía, M. Soldan, J. Sivic, B. Ghanem, and B. Russell, “Temporal localization of moments in video collections with natural language,” *ArXiv*, vol. abs/1907.12763, 2019.
- [203] J. Lei, L. Yu, T. L. Berg, and M. Bansal, “Tvr: A large-scale dataset for video-subtitle moment retrieval,” in *ECCV*, 2020.
- [204] J. Lei, T. Berg, and M. Bansal, “mTVR: Multilingual moment retrieval in videos,” in *ACL*, 2021.
- [205] L. Li, Y.-C. Chen, Y. Cheng, Z. Gan, L. Yu, and J. Liu, “HERO: Hierarchical encoder for Video+Language omni-representation pre-training,” in *EMNLP*, 2020.
- [206] B. Zhang, H. Hu, J. Lee, M. Zhao, S. Chammas, V. Jain, E. Ie, and F. Sha, “A hierarchical multi-modal encoder for moment localization in video corpus,” *ArXiv*, vol. abs/2011.09046, 2020.
- [207] H. Zhang, A. Sun, W. Jing, G. Nan, L. Zhen, J. T. Zhou, and R. S. M. Goh, “Video corpus moment retrieval with contrastive learning,” in *SIGIR*, 2021.
- [208] S. Maeoki, Y. Mukuta, and T. Harada, “Video moment retrieval with text query considering many-to-many correspondence using potentially relevant pair,” *ArXiv*, vol. abs/2106.13566, 2021.
- [209] S. Paul, N. C. Mithun, and A. K. Roy-Chowdhury, “Text-based localization of moments in a video corpus,” *IEEE TIP*, vol. 30, 2021.
- [210] Z. Hou, C.-W. Ngo, and W. K. Chan, “Conquer: Contextual query-aware ranking for video corpus moment retrieval,” in *ACM MM*, 2021.